UNIVERSITY OF CALIFORNIA
SANTA CRUZ

INVESTIGATING MECHANISMS OF ORGANIZATION IN THE EUKARYOTIC GENOME

A dissertation submitted in partial satisfaction
of the requirements for the degree of

DOCTOR OF PHILOSOPHY

in

MOLECULAR, CELL AND DEVELOPMENTAL BIOLOGY

by

Omar Y. Hamdani

June 2017

The Dissertation of Omar Y. Hamdani is approved:

_____
Professor Rohinton Kamakaka, chair

_____
Distinguished Professor Susan Strome

_____
Associate Professor Needhi Bhalla

_____
Tyrus Miller
Vice Provost and Dean of Graduate Studies

Table of Contents

List of Figures and Tables

Abstract

Omar Hamdani

Investigating Mechanisms of Organization

in the Eukaryotic Genome

The eukaryotic nucleus is organized in a non-random, organized fashion. The organization of chromosomes has been found to have a large influence on a diverse set of processes ranging from gene regulation to cell division. These processes are critical to the survival of all living organisms. However, much is still unknown about the principles and mechanisms that are responsible for organizing the genome. The goal of this manuscript is to determine mechanisms that are responsible for organizing the genome.

In mammalian cells, we provide evidence to show that a DNA repair protein, γH2AX, is reproducibly deposited throughout the genome in undamaged cells. Our data also suggest that γH2AX is preferentially found in silenced areas of the genome.

In budding yeast, we show that tDNAs have an effect on chromosome structure. Our data indicate that tDNAs have a role in SMC protein binding, centromere clustering, chromosome mobility, and gene silencing. Furthermore, these effects seem to be mediated locally to the regions surrounding tDNAs.

Dedication and Acknowledgements

I dedicate this PhD to my mother for showing me how to accept people for who they are, to my father for instilling pride in everything I do, my brother Adam for being there no matter what, and my wife Leah for helping me through some of my most difficult times.

I would like to acknowledge the rest of my family and friends for their support throughout my studies.

I would like to acknowledge Rohinton Kamakaka and Namrita Dhillon for the mentorship they provided throughout my PhD, and the rest of my lab members for their help and support.

Chapter 2.2 of this dissertation is the result of collaboration between multiple labs across the world. I'd like to acknowledge the Oki lab for their work on the single cell expression analysis, the Clark lab for their work on the MNase-seq, the Rando lab for their work on the Micro-C, and the Bloom lab for their work on the MSD analysis.

Chapter 1.1: A Review of DNA Repair in the Eukaryotic Nucleus

Histone Modification in DNA Repair

Chromatin is composed of DNA wrapped around a protein complex known as a nucleosome. A nucleosome is made up of a protein octamer composed of histone variants H2A, H2B, H3, and H4. Two molecules of both histones H2A and H2B form two heterodimers that then interact with an H3/H4 tetramer to form a nucleosome. Each histone in the octamer has a globular domain that is essential for the heterodimerization. The histones also have unstructured N- and C-terminal tails that are sites of post-translational modification. In budding yeast, the histone H2A possesses an extended C-terminal tail. This tail includes a phosphorylation site at serine 129 that has an important role in the homologous recombination (HR) mediated DNA double strand break (DSB) repair response [1-4]. In budding yeast, serine 129 phosphorylated H2A is referred to as γH2A. In higher eukaryotes, such as mammals, histone H2A has diverged into both H2A and an entirely different histone protein known as H2AX. Human histone H2AX exists as a single gene on chromosome 11, called H2AFX [3]. H2AX also has an extended C-terminal tail that is phosphorylated on serine 139 by the ATM/ATR kinase (Tel1/Mec1 in *S. cerevisiae*). Phospho-H2AX is called γH2AX. The initial response to a DNA DSB in the HR mediated DNA repair pathway in humans largely mirrors that in budding yeast. The Mre11, Rad50, Nbs1 (MRN) complex will recognize the broken ends of an incurred DNA DSB and recruit the ATM/ATR kinase [5, 6]. ATM/ATR will phosphorylate H2AX at S139 in the area of the DNA DSB leading to γH2AX

deposition. γH2AX will then act as a scaffold for many of the subsequent proteins in the HR pathway leading to the eventual repair of the DNA DSB. This process has been extensively reviewed elsewhere [5, 7, 8].

The γH2A histone mark is conserved across all mammalian species that have been analyzed [3]. Evidence for the presence of histone variant H2AX in higher eukaryotes was first presented in 1980, where H2AX was identified as a different histone variant based on its variant migration from histone H2A [9]. However, the function of γH2AX in DNA repair was not reported until over a decade later [10]. The histone variant H2AX and its function have also been conserved in invertebrate species, such as *D. melanogaster*. In the fly, H2AX is known as H2AV. H2AV differs from H2AX functionally as it has assumed the roles of both γH2AX and another histone variant called H2AZ. H2AZ serves functions in both transcriptional regulation and the DNA damage response in both yeast and humans. However, this histone variant is not the focus of this review, and has been reviewed elsewhere [11]. It is important to note that the function of γH2AX in DNA repair is conferred through a well-conserved 4 amino acid motif at the C-terminal end of the H2AX variant. This SQ[E/D]Φ motif is defined by a serine residue 4 amino acids from the C-terminus of the H2AX histone protein. This will be the serine that is phosphorylated by the ATM/ATR kinase to produce γH2AX [12]. Since the discovery of γH2AX in 1999, γH2AX has been predominantly used as a marker for DNA DSBs [10, 13-15]. However, we have shown that γH2A has functions beyond DNA repair in budding

yeast [1]. Therefore, it is important to interpret past results in the context of other possible functions for γH2AX.

Organizational Characteristics of DNA Repair Proteins

We have recently shown that the DNA repair machinery play a role in the organization of heterochromatin in yeast. DNA repair machinery is well conserved across evolutionarily diverged species. In larger eukaryotes, the DNA damage response includes a much larger and complex cascade of proteins than in budding yeast. This could add multiple layers of redundancy and complexity to any roles that HR mediated DNA repair proteins may play in chromatin organization [7, 8]. By looking to the literature, we may find clues as to whether DNA repair proteins do play a role in genomic organization.

Estimates of the abundance of H2AX in the genome lead to a general consensus of it being present in about 10% of all nucleosomes throughout the genome [10]. While its relative abundance compared to canonical histone variants is known, the distribution of H2AX in the human genome is largely unknown. It has been observed that in response to a DNA DSB, γH2AX spreads in megabase-wide domains flanking the DNA DSB [13]. This result led investigators to use high-resolution (4Pi) microscopy to attempt to explain what may limit the spread of γH2AX [16]. The authors were able to show that non-phosphorylated H2AX is situated into clusters within the nucleus. Upon exposure to a DNA damaging agent, H2AX in the area of a DNA DSB will become phosphorylated to produce γH2AX. The authors speculated that it is the pre-deposited H2AX clusters that determine the spread of γH2AX in

response to damage. This intriguing mechanism suggests that γH2AX is only allowed to spread until a gap in H2AX substrate occurs, at which point the γH2AX spread will end. Building on this result, a recent study has also sought to determine how γH2AX spreading may be limited. Using a genome-wide ChIP-chip approach it was shown that γH2AX may also be limited to its domain around DSB's by the tethering molecule cohesin [15]. By using an inducible restriction enzyme DNA DSB system, the authors show that in the area around a DSB, γH2AX is depleted in regions where cohesin peaks. It appears that while cohesin is necessary for proper DNA repair, cohesin may also be refractory to the spread of γH2AX in certain contexts.

Outside of *HMR* in *S. cerevisiae*, a tDNA acts as an insulator to block the spread of heterochromatin [1]. This tDNA is enriched for Scc2, the cohesin and condensin loading complex, and both cohesin and condensin. γH2A is present at the silent *HMR* domain, and extends to the tDNA suggesting that the tDNA aids in blocking the spread of both γH2A and silencing proteins [1]. γH2A is also necessary for the interaction of the silent *HMR* and *HML* domains. Furthermore, establishment of silencing at *HML* and *HMR* is dependent on γH2A deposition. These results suggest that γH2A functions to mediate silent interactions and establish silent chromatin domains in budding yeast. If γH2AX is serving a similar function in mammalian cells, we can predict that highly transcribed and cohesin bound genes in larger eukaryotes may act as a barrier to the spread of silencing. We can also predict that γH2AX will colocalize with silencing proteins throughout the nucleus.

Interestingly, we do find tDNAs and cohesin bound genes at physical domain borders between silent and active chromatin in higher eukaryotes [4, 17]. However, γH2AX has not been shown to colocalize with silencing proteins in undamaged mammalian cells. We must now ask the question, where do we find γH2AX in undamaged cells?

Heterochromatin bound γH2A in budding yeast has been shown to play a role in mediating and/or stabilizing interactions between heterochromatic loci in undamaged cycling cells [1, 18]. However, does γH2AX play a similar role in higher eukaryotes? To date, there has been no attempt to map the location of γH2AX in undamaged mammalian cells. However, in yeast and *Drosophila* γH2A is present at heterochromatic loci [2, 19, 20]. In addition, in budding yeast DNA damage repair proteins are constitutively bound at the telomeric loci. The Ku70/80 complex is preferentially bound to telomeres and is necessary for proper telomere fidelity [21]. This function appears to be conserved in humans where Ku binds telomeric loci to protect chromosome ends [22]. Considering that the same DNA repair proteins from both yeast and flies are conserved in higher eukaryotes, we can predict that HR mediated DNA DSB repair proteins could play a similar role in the heterochromatic structure of higher eukaryotes.

Silencing in the DNA DSB Damage Response

Recent studies have shown that there is a significant interplay of proteins within the HR mediated DNA DSB response pathway and silencing machinery. It has been observed that in the area surrounding a DNA DSB histone H2A and H2AX display significant levels of ubiquitination [23]. Ubiquitination of histone H2A has

been linked to polycomb-dependent silencing, and a 2010 a study chose to ask whether H2A ubiquitination in the DNA damage response might also play a role in silencing regions that flank DNA DSBs. The system that was used involved inducing a DNA DSB upstream of a reporter gene. This study showed that, in response to an induced DNA DSB, silencing of a downstream reporter gene in cis to the break occurs. Furthermore, this silencing was dependent on the activity of the ATM kinase and E3 ubiquitin ligase activity [24]. ATM is responsible for the production and spread of γH2AX in the area of a DNA DSB, but is γH2AX necessary for the silencing observed in this system?

The authors of a more recent study examined the recruitment of polycomb silencing machinery to micro-laser induced DNA DSB's. As expected, when DNA DSBs are induced, γH2AX is clearly deposited in the area of the break on the chromosome. However, the authors also show that polycomb proteins colocalize with the domains of γH2AX that mark DNA damage. Additionally, ChIP-qPCR within the region surrounding an induced DNA DSB has shown that polycomb proteins localize in the area of DSBs. Furthermore, polycomb protein recruitment is dependent on the ATM/ATR kinase and E3 ubiquitin ligase activity [25]. Taken together, these data suggest an important role for silencing machinery in HR mediated DNA DSB repair pathway.

Polycomb group proteins are not the only silencing proteins that show an association with DNA repair proteins in higher eukaryotes. A study done in 2008 showed that KAP1, a heterochromatic adapter protein, acts as a barrier to the

resolution of a subset of DNA DSBs [26]. Importantly, the resolution of these DNA DSBs was dependent on the ATM kinase. The study is not without flaws. For example, the study was done in contact inhibited MEFs which are mostly in G1 of the cell cycle. The predominant repair pathway during G1 is non-homologous end joining (NHEJ) [8]. However, HR mediated repair is primarily used after DNA replication in G2/M phase. Therefore, the authors were looking at HR proteins in a part of the cell cycle where HR mediated repair is not the predominant mechanism of repair. The authors also use γH2AX as a mark of unrepaired DSBs. However, there is no attempt made to discern whether the γH2AX foci that colocalize with dense heterochromatic foci (chromocenters) are unrepaired DNA breaks, or whether the γH2AX that has been deposited in the area simply hasn't been evicted after break resolution. While there are some caveats to think about from the results in this paper, it does provide president to show that there is a dynamic interplay of silencing and HR proteins in higher eukaryotes.

We also find that heterochromatin acts as a barrier to DNA DSB resolution in *Drosophila melanogaster*. In 2011, a group investigated the dynamics of DNA DSB repair in the chromocenters of *Drosophila* Kc cell nuclei [27]. An important point to make about this cell line is that Kc cells are embryonically derived, and spend a majority of their time in S/G2 of the cell cycle. During G2/M phase of the cell cycle, HR machinery is predominantly responsible for repair of DNA DSBs [28]. This makes Kc cells an excellent candidate for the study of HR mediated resolution of DNA DSBs in heterochromatin. As was mentioned earlier, the function of γH2AX is

conferred through the histone variant H2AV in drosophila. The authors were able to show that when a DNA DSB occurs in a chromocenter, γH2AV is deposited within the chromocenter. However, later steps of repair could only occur outside of the chromocenter (i.e. strand invasion and beyond). Therefore, early steps in the HR repair pathway occur within chromocenters (i.e. γH2AV deposition and DNA resection), and late HR repair steps don't occur until the DSB is moved out of the chromocenter. In corroboration with the Goodarzi result, the authors also show that HP1 and its associated proteins act as a barrier to the production of marks for strand invasion inside chromocenters, as denoted by colocalization of the late stage repair protein Rad51 foci with chromocenters. Surprisingly, we also find that heterochromatin cannot be established properly in mutants that are deficient for histone H2AV [29]. These results show that in different contexts silencing proteins can either facilitate or inhibit the repair of DNA DSBs through the HR pathway in higher eukaryotes.

The Role of γH2AX in Genome Stability and Organization

The point of this section is to raise questions and possible avenues of investigation for the study of the role γH2AX and other repair proteins in mechanisms of genome organization.

Past study has found that replication in mammalian cells takes place in spatio-temporal domains [30]. Domains that replicate early on in S phase tend to be more highly transcribed, while domains that replicate late in S phase tend to be less transcriptionally active [31]. Barrier to replication forks include origins of

replication, heterochromatic loc, and highly transcribed genes. At both stalled and collapsed replication forks in mammalian cells we find γH2AX deposition. At stalled forks it's thought that ATR is the predominant kinase that phosphorylates H2AX, while at collapsed forks ATM takes over [32]. A recent study took advantage of known barriers to replication, and identified the location of fragile sites that are prone to breaks in the genome of murine b cells [14]. This is one of the lone genome wide distributions of γH2AX available from the literature in mammalian cells. It is important to note that in order to capture these ERFS's the authors stimulated B cells into proliferation and then arrested them in early S phase with hydroxyurea (HU). This paper presents no information on the distribution of γH2AX in unperturbed mammalian cells. However, we do uncover some interesting observations from the data. The authors find that both replication fork proteins and γH2AX colocalize in a reproducible fashion throughout the genome upon HU treatment at several different types of loci. Most notably we find γH2AX deposition at transposable elements, tDNAs, and rDNA loci. Comparing this information to what we have learned in yeast, we find that all of these loci act as a barrier to replication in both *S. cerevisiae* and *S. pombe* respectively [2, 19]. Are these loci also bound by γH2AX in unperturbed cycling cells, or does any binding of γH2AX denote replication fork stalling or collapse? The fact that γH2A is necessary for clustering of heterochromatic loci in *S. cerevisiae* throughout the cell cycle suggests that the function of γH2A in budding yeast provides function beyond stalled forks [1, 18]. Alternatively, in higher eukaryotes γH2AX may only be deposited in the event of a

stalled/collapsed fork, and H2AX may be present at areas that are more prone to fork stalling/collapse. This hypothesis has not been tested, and to date no study has conducted a genome wide survey of H2AX in unperturbed, cycling human cells.

Going far back in the literature we find evidence that γH2AX may be overrepresented in heterochromatic fractions of chromatin. In 1978, a biochemical fractionation study was done in two different species of deer mouse cells [33]. In this study, the rate of $^{33}PO_4$ incorporation was used to measure the steady state level of phosphorylation among each histone variant. Interestingly, in heterochromatic fractions histone H2A (likely H2AX, as it had not been discovered yet) was more highly phosphorylated when compared to non-heterochromatic cell fractions. This result suggests that γH2AX may be present at heterochromatic loci, but it provides no information on the function γH2AX may serve in heterochromatic fractions of chromatin.

Little to no information exists in mammalian cells on what role γH2AX may play in undamaged human cells. This leaves us with a list of open questions that could help us determine the function γH2AX in undamaged mammalian cells: Do DNA repair proteins have some role in mediating interactions within the mammalian nucleus? Are DNA repair proteins reproducibly deposited at specific loci in the genome of undamaged mammalian cells? Are areas where we find γH2AX deposition simply due to replication stress, or does γH2AX serve some function other than repair at these loci. Future experimentation should seek to answer these questions. These experiments could lead to information about pathways involved in genomic

interaction, and a significant understanding of the basic principles that govern nuclear architecture could be uncovered.

Chapter 1.2: Non-Canonical Roles for DNA Repair Proteins in Mammalian Cells

Omar Hamdani[1], Namrita Dhillon[1], and Rohinton Kamakaka[1]

1 Department of MCD Biology**,** 1156 High Street, University of California, Santa Cruz, CA 95064 USA

Introduction

The eukaryotic genome is organized in a non-random and orderly fashion. Specific interactions within chromosome segments occur in a predictable and reproducible manner from one cell to another [4, 17, 34-36]. Chromatin interactions play a role in transcriptional activation, such as enhancer-promoter interactions at transcription factories [37, 38]. Interactions can also be based on silencing, such as long-range interactions at polycomb bodies and telomere-telomere association at the nuclear periphery [21, 39]. These long-range interactions are observed across eukaryotes of all types, but many of the proteins and factors that determine the architecture of the genome are not known.

In budding yeast, we have shown that γH2A deposition is necessary to drive interactions between the heterochromatic loci *HML* and *HMR* [1]. *HML* and *HMR* act as barriers to replication, as ascertained through DNA pol epsilon mapping, indicating that replication forks pause at these sites. Stress is induced on the DNA through paused or stalled replication forks, and this activates the HR mediated repair pathway. In mammalian cells, many of the common fragile sites appear to be replication stress sites since they share many of the same characteristics as fork barriers in yeast [40]. Studies in budding yeast have shown that highly transcribed genes, heterochromatin,

origins of replication, and transposable repeat elements act as barriers to DNA replication. These same genomic elements act as barriers to replication in human cells as well, and these sites efficiently recruit γH2AX following exposure to DNA damaging agents [14, 41]. This provides precedent for the idea that γH2AX may play a similar role in human cells. It is important to note that all human studies that have mapped γH2AX to date have only mapped γH2AX in response to DNA damage. Genome wide mapping of γH2AX in undamaged cells has not been done. Furthermore, our lab has shown that ectopic recruitment of HR repair proteins can silence a reporter gene by interacting with and recruiting repressor proteins in budding yeast [18]. Therefore, it is possible that γH2A is deposited simultaneously with silencing proteins on the chromatin as a preemptive strategy to deal with replication stress at heterochromatin. Alternatively, γH2A could be deposited in response to inevitable replication stress. Irrespective of which model is correct, it is evident that in yeast γH2A is playing a role in the establishment and maintenance of silencing in yeast.

All of the proteins that are found to be involved in HR protein recruitment to silent chromatin in budding yeast are conserved in humans [7, 8]. There is also evidence to show that silencing and DNA repair are co-dependent processes even in mammals. In response to a double strand break, silencing spreads in cis along chromosome arms flanking a DNA DSB [24]. DNA DSB induced silencing is dependent on the ATM kinase, one of two redundant kinases that phosphorylate histone H2AX to create γH2AX. The spread of silencing to distal areas flanking

DNA DSBs is similar to the megabase wide spread of γH2AX on the chromatin flanking DNA DSBs [16]. We also silent chromatin can be refractory to repair, but not to the deposition of γH2AX. When a DNA DSB occurs in heterochromatin, γH2AX is deposited in the area of the break. However, the break is unable to be completely repaired until the chromatin is relaxed, and the site of damage is moved outside of the heterochromatic foci [26]. Relaxation of the heterochromatin is dependent on the ATM kinase, which phosphorylates the heterochromatin adapter protein KAP-1. Once phosphorylated, KAP-1's association with heterochromatic factors, such as HP1, is perturbed and the chromatin is allowed to relax leading to the resolution of the DNA DSB. These studies establish precedent to show that HR proteins show a strong association with silencing machinery in mammalian cells. Therefore, it is possible that γH2AX, like γH2A, plays a role in silencing and silent interactions in the human nucleus.

We propose that HR mediated DNA DSB repair proteins play a conserved role in mediating heterochromatic interactions, and establishment of silencing in human cells. In this study we show that γH2AX is reproducibly enriched in undamaged human cell lines. We also show evidence that suggests that γH2AX is preferentially associating with heterochromatic loci throughout the genome.

Results

γH2AX is detectable in undamaged mammalian cells by immunofluorescence microscopy and western blot

γH2AX is traditionally known as a mark of DNA DSBs, and has been used for this purpose in most of the published literature. In all of these experiments, cells were subjected to some type of DNA damaging agent, and γH2AX was used to assay the extent of the damage that occurred. However, we are proposing that γH2AX could also have other functions in the genome of human cells. The first logical step to prove that would be to determine if γH2AX is present in undamaged human cells. We first sought to determine if γH2AX is present in undamaged normally cycling human cells using immunofluorescent (IF) microscopy of fixed human HEK293FT cells. Two treatment groups of cells were used. One set of cells was irradiated with 160 Kv (6.2 mA) x-rays for 3 minutes, and a second set of cells were treated in the same manner as the irradiated cells without being subjected to x-rays as a control. Cells were then put at 37C with 5% CO2 for recovery, and were fixed at 30 minutes and 60 minutes post-irradiation. Fixed cells were subsequently blocked in blocking buffer containing goat serum and incubated with a primary antibody specific to the phosphorylated γH2AX histone mark. After incubation with a secondary GFP antibody, the cells were placed on slides using mounting media with DAPI stain, and imaged using a wide-field fluorescent microscope at 40X magnification.

The top 2 panels in figure 1 show 293FT cells that have been irradiated and allowed to recover for 30 minutes and 60 minutes respectively. The lower panel is an non-irradiated sample that has been imaged against γH2AX. At both 30 minutes and 60 minutes after irradiation, large GFP foci are detected within the nuclei of damaged cells. When compared to the control image, both irradiated images display a

significantly increased number of GFP foci. Furthermore, GFP foci in damaged cells appear to be larger than the control cell GFP foci. This result suggests that the γH2AX antibody that was used for immunofluorescence was specific to an epitope that increased in concentration in response to DNA damage. Considering the role of γH2AX plays in DNA repair, this provides evidence to show that our antibody is specific to γH2AX. Most importantly, in the non-irradiated cells we still see γH2AX foci. This result suggests γH2AX is present in cells that have not been subjected to DNA damaging agents.

To further investigate whether γH2AX is present in unperturbed human cells, we next used an U2OS cancer cell line with a stably integrated inducible AsiSI restriction enzyme. Upon addition of 4-hydroxytamoxifen (4OHT) to cell media, the AsiSI enzyme is expressed and will cut DNA at its 8 bp recognition sequence throughout the genome [15]. This leads to the production of DNA DSBs throughout the genome. The restriction enzyme contains an HA tag in order to monitor for the expression of the AsiSI restriction enzyme. As a control, the same U2OS-AsiSI cell line was treated with DMSO as mock treatment. Cells were treated 4OHT or DMSO, incubated 4 hours to allow for expression of AsiSI, fixed, stained, and imaged as was described in the previous experiment.

Split channel images for both 4OHT and mock treated cells, along with a merged image, are displayed in figure 2. Mock treated image panels are shown on the top portion of the figure. Image panels are displayed as DAPI, HA-AsiSI, and γH2AX moving from left to right. The merged imaged for each treatment group is

shown above and below their respective row of split channel images. The panels displaying HA-AsiSI images show that 4OHT treated cells display a more intense RFP staining when compared to control cells. This result suggests that the AsiSI enzyme is more highly expressed in 4OHT treated cells compared to control cells. The 4OHT treated cells also displayed a larger number of large GFP foci in response to AsiSI induction when compared to control cells. This result suggests that γH2AX formation occurs in the area of DNA DSBs created by AsiSI. Importantly, we observe a significant number of γH2AX foci in mock treated cells. Taken together, these results suggest that, after the induction of AsiSI expression, DSBs are created throughout the genome. Importantly, there is also a significant detection of γH2AX in cells prior to DNA damage.

We have shown that γH2AX is detectable by immunofluorescence in two different types of cell lines that have not been subjected to DNA damaging agents. To further confirm that γH2AX is present in undamaged cells, we wanted to determine if γH2AX is present in cells before and after DNA damage by western blot. Using a western blot as an alternative to IF for γH2AX detection will also provide details on the size of the protein that our γH2AX antibody recognizes. Histone proteins have a size corresponding to ~15 kd on a western blot. Therefore, we would expect to see a band of around 15 kd when blotting is done for γH2AX. In order to carry this experiment out, we created cell lysates from both HEK293FT and U2OS-AsiSI cell lines. HEK293FT cells were treated with x-ray irradiation in order to induce damage and extracts were prepared. Irradiation efficiently induces a dose

dependent γH2AX response. Irradiated HEK293FT were used as a positive control in this experiment because we had previously shown that x-ray exposure induces an acute dose-dependent γH2AX increase in HEK293FT cells (data not shown). Cell lysates were also prepared from U2OS-AsiSI cells that had been induced with 4OHT treatment, or U2OS-AsiSI cells that had received a mock treatment. For sample preparation, cells were counted prior to harvesting, and approximately equal numbers of cells were used to prepare cell lysates. Crude lysates were prepared by boiling freshly harvested cells in 1X Laemmli buffer + DTT for a period of 5 minutes. Equal volumes of lysate were then loaded and separated on a 15% SDS-PAGE, and subsequently electro-transferred to PVDF membranes. Membranes were incubated with the same primary γH2AX antibody used in our immunofluorescence experiments, and visualized through an HRP-coupled secondary antibody. Membranes were also incubated with a primary antibody against γTubulin as a loading control.

In the left panel of figure 3, the results from the γH2AX blots are shown, and in the right panel the γTubulin loading control is shown. U2OS-4OHT, U2OS-mock, and irradiated 293FT cells were loaded into lanes 1, 2, and 3 respectively. A band corresponding to a size of ~15 kd was detected in lanes 1 and 3. This band was not found in lane 2, where undamaged cell lysates were loaded. There are also bands detected from 20 to 25 kd in lane 3. The identity of the 20-25 kd bands are unclear. The γTubulin blot shows 2 bands of approximately equal intensity in both lane 1 and 2, U2OS 4OHT/mock, at ~50 to 60 kd. In the third lane, containing the irradiated

293FT cells, these two bands are present at a higher intensity. The expected size of γTubulin is ~60 kd. These results suggest that while both U2OS groups have approximately equal amounts of protein loaded, more irradiated 293FT protein lysate was loaded onto the SDS-PAGE than either U2OS group. Other unexpected bands are present at 15 kd in lanes 1 and 3, and 20 kd in lane 3. We attribute these bands to cross reactivity that could have occurred when both blots were washed together after primary antibody incubation. Taken together, the results from our western analysis suggest that γH2AX is detected only after exposure to DNA damaging agents. However, we do note at lower times of exposure, a 15 kd band was detected in the lane containing undamaged U2OS-AsiSI lysates (data not shown). This suggests that γH2AX is detected by western analysis in undamaged human cells.

γH2AX is detectable in undamaged human cells by immunoprecipitation

γH2AX appears to be present in undamaged human cells, as shown by IF and western blot analysis. The ultimate goal of our approach is to determine where γH2AX bound throughout the genome. Our reasoning was that by determining if γH2AX is reproducibly found in a certain chromatin environment, this could provide clues on whether γH2AX has function outside repair. We planned to use chromatin immunoprecipitation (IP) sequencing (ChIP-seq) to map γH2AX throughout the genome. In order to ChIP γH2AX, we had to first show that γH2AX could be immunoprecipitated (IP'd) from undamaged human cells. If a protein can be pulled down efficiently in an IP, the general rule is that ChIP of that same protein will work. Given this information, we chose to do an IP of γH2AX in undamaged HEK293 cells

followed by western blot for visualization. In preparation, 293 cells were harvested and immediately lysed in SDS buffer containing protease inhibitors. Cells were then subjected to cup horn sonication, diluted in IP buffer, and spun at high speed to clear cellular debris. At this point, aliquots were removed to be used as crude extract before IP. IPs were done overnight at 4C using either a γH2AX or HA antibody. The HA antibody IP served as a control for specificity of the γH2AX antibody used in the IP. After the overnight incubation, antibody-bound epitopes were pulled down using a protein A/G slurry, washed in IP buffer, boiled in 1X Laemmli buffer, and spun down. The supernatant containing the IP'd proteins was then loaded onto a 15% SDS-PAGE for separation, and western blots were done as previously described. A different γH2AX antibody than the IP γH2AX antibody was used during primary incubation of the membranes. A control western blot was also done on crude lysates with γTubulin as a loading control. All samples on the γH2AX blot were loaded in duplicate with volumes of 7.5 and 15 μl respectively.

The left panel of figure 4 shows the γH2AX blot, and the right panel shows the γTubulin blot. A band of approximately equal intensity is detected at ~50 kd in the Tubulin blot for both γH2AX and HA crude extracts suggesting approximately equal amounts of protein were used in both the γH2AX and HA IPs. The γH2AX panel shows the presence of multiple bands. γH2AX is expected to show up as a molecular size of ~15 kd, similar to the size of other histone variants. In both crude extracts used for the IP (lanes 1-2 and lanes 5-6), a band is present at ~15 kd. This band is also present after IP with γH2AX, but is not seen after IP with an HA

antibody. These results suggest that γH2AX is present in the crude lysate prepared from undamaged HEK293 cells. After IP's were done, we now see that the ~15 kd band that likely corresponds to γH2AX is not present in the HA IP but is present in the γH2AX IP. This result suggests that we successfully IP'd γH2AX protein in undamaged cells. Furthermore, the antibody used for the γH2AX IP was specifically recognizing γH2AX. Lastly, bands present at 20 and 25 kd in both IP samples likely correspond to the constant domain of the antibody that was used to perform the IP, since the band is detected in both IP samples and not in the crude lysate. Taken together, these results show that we were able to successfully IP and detect γH2AX in undamaged HEK293 cells.

γH2AX is detected heterochromatic fractions of the nucleus

Previously we showed that, in budding yeast, γH2A plays a role in driving the interaction between heterochromatic loci [1]. In order to determine if the role γH2A plays in heterochromatic interaction is conserved in human cells, we carried out cellular fractionation followed by western analysis to detect whether γH2AX is present in heterochromatic fractions of the nucleus. The first step in our assay was to prepare intact nuclei from HEK293 cells. HEK293 cells were harvested and subjected to dounce homogenization in two steps. First, a loose dounce pestle was used for the initial cell lysis. The lysate was then centrifuged at high speed, pelleted, and resuspended. Second, a tight dounce was used until complete homogeneity was confirmed. The lysate was then layered onto a sucrose cushion and separated by centrifugation. The pellet containing the nuclei was resuspended. Isolated nuclei

were subjected to MNase digestion, and aliquots were taken at five different time points during the 20-minute MNase treatment. MNase will cut DNA in the linker DNA between nucleosomes. Therefore, more open and accessible chromatin will be digested before dense constrained chromatin [42]. We next isolated three separate fractions of chromatin: S1 (soluble mononucleosomes), S2 (long, soluble chromatin), and P (nuclear matrix associated chromatin). The S1 will contain open chromatin that was easily accessed by the MNase, and spins out of the lysate without nuclear lysis. S1 corresponds to a euchromatic fraction. The S2 contains long, soluble chromatin that is cut by the MNase less efficiently due to constrains in its chromatin structure, and spins out of the lysate after nuclei have been lysed in EDTA. S2 corresponds to a soluble chromatin fraction with significant amounts of heterochromatin. Lastly, the remaining pellet P contains chromatin that remains associated with the nuclear matrix. This corresponds to laminar-associated heterochromatin at the nuclear periphery. Fraction P was immediately resuspended in 1X laemli buffer and boiled for 5 minutes to prepare the lysates for western analysis. In order to isolate soluble protein from both S1 and S2, TCA precipitation was carried out. Lysates from each fraction for all five time points were then separated on a 15% SDS-PAGE, and transferred to membranes for blotting and visualization with an antibody against γH2AX and non-phosphorylated H2AX. γH2AX blotting allowed us to determine where γH2AX fractionates in the nucleus, and H2AX blotting allowed us to determine if the γH2AX mark is deposited differentially among H2AX histone

monomers. We also extracted DNA from lysate at each time point in order to monitor the digestion of chromatin due to MNase treatment.

As a control, we prepared DNA from each fraction at each time point. This DNA was separated and visualized by agarose gel electrophoresis (Figure 5). After two minutes of MNase treatment, bands are detected at ~200 bp's proceeding up in 200 bp steps. Nucleosomes are spaced throughout the genome in approximately 200 bp increments [42]. This result suggests that MNase is efficiently cutting linker DNA to produce free mononucleosomes. Bands appearing at 400, 600, and 800 bp are representative of DNA associated with two, three, and four nucleosomes respectively. This pattern extends up the length of the lane. After 10 minutes of MNase treatment, there is a shift from dark bands being present along the entire length of the lane at the 2-minute time point to an increase in intense bands observed at 200 bp's. This result suggests that as the MNase treatment proceeds a larger portion of the linker chromatin is being digested, and the mononucleosomal fraction of DNA on the gel is increasing as a result. Importantly, by 10 minutes the reaction is proceeding to completion.

The left panel of figure 6 shows a western blot against γH2AX. At the 0 time point, an intense band at 15 kd is found only in the P fraction. At this point, the nuclei have not undergone MNase treatment, and should be largely intact. This result suggests that the majority of γH2AX is found in the nucleus before MNase digestion. By 2 minutes after MNase digestion, a feint band is produced in the S1 fraction at 15 kd along with a more intense band in the P fraction. This result suggests that a small

amount of γH2AX is detected in free mononucleosomes after 2 minutes of MNase digestion. 5 minutes after MNase digestion, an intense 15 kd band is detected in the S2 fraction, along with a feint band in the S1 and intense band in P at 15 kd. This result suggests that most γH2AX is found in long, soluble chromatin and in association with the nuclear matrix after 5 minutes of MNase treatment. This banding pattern remains the same at both the 10 and 20-minute time points as the MNase reaction proceeds. The most intense bands are produced in both the S2 and P fractions, which suggests that γH2AX preferentially associates with soluble heterochromatin and laminar associated domains. Taken together, these results suggest that γH2AX is detected at a higher level in both soluble heterochromatin and laminar associated heterochromatin when compared to euchromatic fractions.

The right panel of figure 6 shows a western blot that was done with an antibody designed against non-phosphorylated histone H2AX. At the 0 time point, a band is detected in the P fraction at 15 kd just as was seen in the γH2AX blot. This result suggests that chromatin has not been digested in order to release soluble chromatin. After two minutes, bands are present at 15 kd in all three fractions. This banding pattern remains constant at both the 5 and 10-minute marks. These results suggest that H2AX is found equally in all three fractions of chromatin after 10 minutes of MNase digestion. We note that the band found in the S1 fraction at 15 kd appears to decrease in intensity after 20 minutes, and we attribute it to an error that occurred while loading the gel. Taken together, these results suggest that H2AX does not show preferential association with a specific type of chromatin.

γH2AX maps to heterochromatic regions across the human genome

We are testing a model that proposes γH2AX may be playing a role in the genome beyond DNA repair. This model predicts that γH2AX will map to specific points throughout the genome in a reproducible manner. In order to test this prediction, we carried out ChIP-seq of γH2AX in undamaged, cycling HEK293 cells. We used HEK293 cells because most of our prior work was done in this cell line. HEK293 cells were prepared and ChIP'd as previously described [43, 44]. In brief, cells were harvested and cross-linked in 1% formaldehyde. Cross-linked cells were lysed in SDS buffer and sonicated using a Diagenode Bioruptor. The size range of the chromatin was confirmed to be ~200-400 bp's, and the sample was diluted in IP buffer. Sonicated chromatin was then incubated over night at 4C in the presence of an antibody specific to γH2AX. Before incubation with the γH2AX antibody, input chromatin was taken from the diluted sample. The next morning antibody-bound epitopes were pulled down from the chromatin sample through incubation with protein A/G beads, and the immuno-complexes were then washed sequentially in high salt and low salt wash buffer respectively. Elution buffer was added to the IP'd chromatin complexes to disrupt protein interactions, and crosslinks were reversed overnight at 65C in the presence of NaCl. The input and IP'd DNA were isolated away from protein through phenyl chloroform extraction. Both input and IP DNA samples were quantified using an Invitrogen Picogreen assay. We then prepared high throughput sequencing libraries using the Illumina Genomic DNA Library Prep Kit.

In preparation for sequencing, the libraries were size selected using the Invitrogen E-gel system. The sizes of all libraries were confirmed by high sensitivity bioanalyzer chip to be between 300 to 500 bp's in length. The finished libraries were paired-end sequenced using an Illumina Hi-Seq 2500. The resulting reads were normalized and mapped to the hg19 human reference genome. Called peaks consisted of any reads in the IP samples that mapped back to the genome at a threefold increase when compared to input. Peaks were called using a 200 bp sliding window, and any called peaks within 600 bps of each other were merged to make one peak.

Figure 7 shows the results of the γH2AX ChIP-seq experiment that was done. First, an abundance of peaks were called on the X chromosome. Only the X chromosome is found in this dataset because the HEK293 cancer cell line was isolated from a female patient. We also note that peaks are found at telomeric loci across the genome. Chromosome 6 shows a specific enrichment of called peaks when compared to all other chromosomes excluding the X chromosome. γH2AX peaks are also found throughout the genome on other chromosomes in smaller number. However, these peaks do not show any association with particular parts of chromosomes. These results suggest that γH2AX is reproducibly enriched across the human genome in undamaged human cells. Enriched loci in undamaged human cells include telomeres, the X chromosome, and chromosome 6.

Discussion

Studies that have investigated the function of γH2AX have traditionally focused on its role in the DNA DSB repair pathway [7, 8, 45]. This study has shown

that γH2AX may have functions within mammalian cells that extend beyond the role of γH2AX in DNA repair. We show that γH2AX is present in undamaged, normally cycling mammalian cells via IF and western analysis. We are also able to IP γH2AX in undamaged mammalian cells. Through cell fractionation, we show that γH2AX may be preferentially associating with heterochromatin. Lastly, γH2AX reproducibly maps to multiple loci throughout the human genome including telomeres, the X chromosome, and along the arms of chromosome 6. Taken together, our results suggest that γH2AX is present in undamaged human cells at predictable loci throughout the genome.

We have shown that γH2AX is present in the human genome at reproducible loci in cells that have not been subjected to DNA damaging agents. However, we currently lack knowledge on the function γH2AX may be playing at these loci. In *S. cerevisiae*, *S. pombe* and *Drosophila melanogaster*, γH2A is found at all heterochromatic loci across the genome [1, 2, 19]. It is thought that this is because condensed heterochromatin acts as a barrier to replication leading to a stalled replication fork and subsequent γH2A deposition. ChIP experiments done to map DNA pol epsilon, a proxy for DNA replication fork progression, have found specific enrichment at heterochromatin in budding yeast. This result suggests that replication forks are actually stalling at heterochromatic sites across the budding yeast genome (data not shown). γH2A and γH2AX are found in yeast and humans at sites throughout the genome that act as barriers to replication and aren't heterochromatic [2, 14, 19]. These other types of replication barriers include tDNAs, origins of

replication, and other highly transcribed genes. One explanation for the reproducible enrichment of γH2AX in the human genome could be that the sites at which γH2AX is found are barriers to replication. At stalled and collapsed replication forks in mammalian cells, HR mediated repair is responsible for fork restart in a RAD51 dependent manner [46]. However, RAD51 recruitment occurs late in the HR pathway during strand invasion. The deposition of γH2AX is one of the earliest steps in the pathway. If γH2AX is found at loci throughout the genome that can act as a barrier to replication, it is possible that γH2AX enrichment in the genome is the result of DNA damage rather than γH2AX playing a role in long-range interaction. However, one explanation does not preclude another. There could be overlap between these two models.

In humans, DNA repair and silencing have diverged in several pathways with many different redundant proteins that are not found in budding yeast. Therefore, it is important to consider that the role of γH2AX may not be exactly the same as the role γH2A plays in budding yeast. Our mapping study found that γH2AX is reproducibly enriched along the X chromosome in human cells. Interestingly, a 2003 study showed that γH2AX is necessary for establishing a dense heterochromatic structure comprised of the X and Y-chromosomes during male meiosis in mice. In mice deficient for production of H2AX, this sex body fails to form [47]. It's possible that the enrichment of γH2AX that we find on the X chromosome may play some role in sex chromosome silencing. We do note that this study found γH2AX to be necessary during male meiosis, while we mapped γH2AX in mitotic female cells. However,

HEK293s are a cancer cell line, and it's entirely possible that ectopic nuclear processes may be operating. Another possibility is that γH2AX plays a more general role pertaining to structure and function of the X chromosome. However, future experiments will need to be done to determine exactly why γH2AX is enriched on the X chromosome.

We have shown that γH2AX is present in undamaged cells at reproducible loci in undamaged cells. However, we do not know what γH2AX is doing at these loci. What proteins does γH2AX physically interact with in undamaged cells? Does γH2AX mediate interactions throughout the genome? Future experimentation should focus on parsing out the answers these questions. This will shed light on the function of γH2AX in undamaged human cells.

Figures

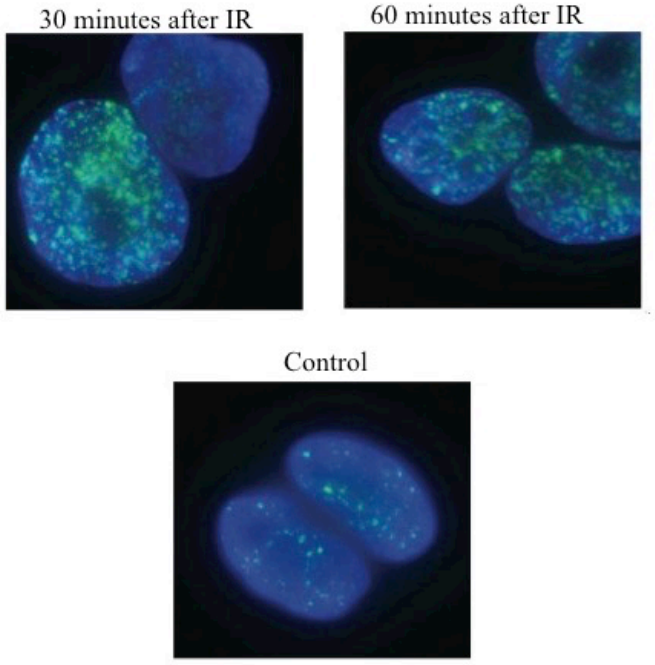

Figure 1. **γH2AX is detected in undamaged HEK293FT Cells by IF.** HEK293FT cells were subjected to 160 Kv X-ray gamma irradiation for a period of 3 minutes. The top two panels show images of cells in recovery at 30 minutes and 60 minutes after irradiation. The control panel is cells treated in exactly the same way as the irradiated cells without being irradiated. γH2AX is shown in green, and the nucleus is marked through DAPI staining in blue.

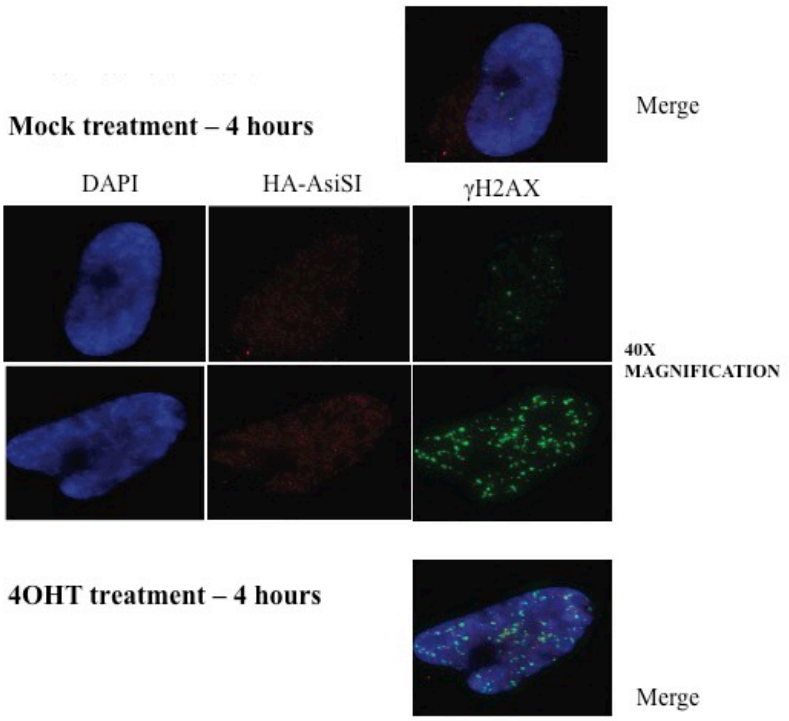

Figure 2. **γH2AX is detected in undamaged U2OS cells by IF.** IF of U2OS cancer cells containing a tamoxifen inducible AsiSI restriction enzyme. Mock treated cells are shown in the top 4 panels, and 4OHT induced cells are in the bottom 4 panels. Split channel images of cells are shown in the middle six panels. γH2AX is shown in green, HA-AsiSI is shown in red, chromatin is shown in blue through DAPI staining. Merged images of each treatment group are also displayed.

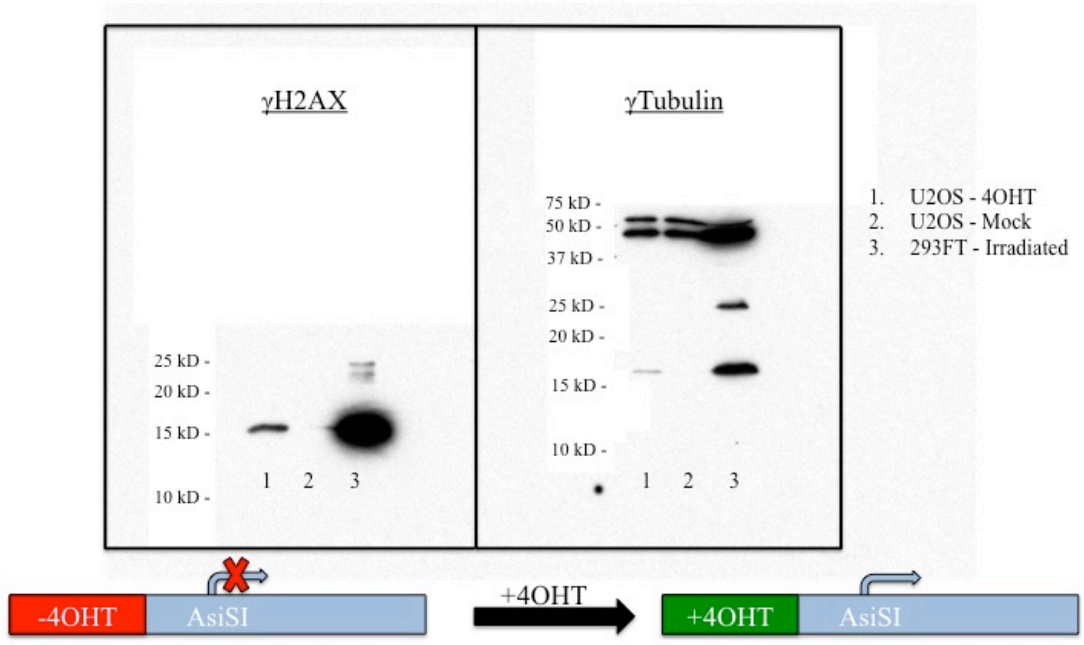

Figure 3. **γH2AX is detected in response to DNA damage by western blot.** Western analysis of irradiated 293FT cells and tamoxifen induced U2OS-AsiSI cells. The left panel shows a western blot done against γH2AX (~15 kD). Lanes 1, 2, and 3 contain cell lysate from tamoxifen induced U2OS cells, mock treated U2OS cells, and irradiated 293FT cells respectively. γTubulin (~50 kD) is shown as a loading control. Molecular weights are shown to the left of each panel. Samples were run on 15% SDS-PAGE for separation.

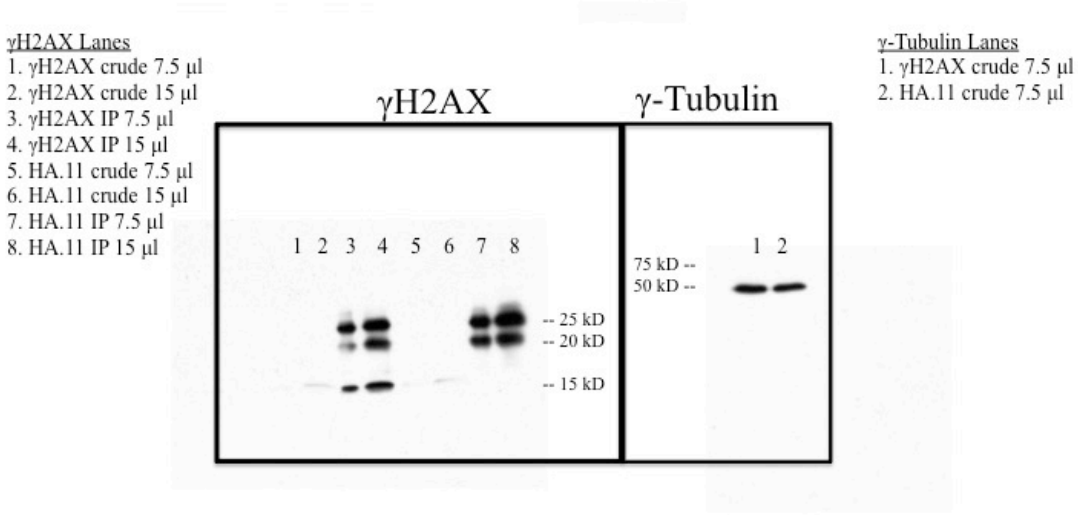

Figure 4. **γH2AX can be immunoprecipitated from undamaged human cells**. I–western analysis of γH2AX in undamaged HEK293 cells. The left panel shows a blot done against γH2AX. The order and identity of each lane are shown to the left and right of each blot. IPs were done using either an antibody specific to γH2AX or an HA antibody as a control for non-specific pull-down. γTubulin is shown as a loading control. Molecular weight markers are found to the right of the γH2AX blot and to the left of the γTubulin blot. Samples were run on a 15% SDS-PAGE for separation.

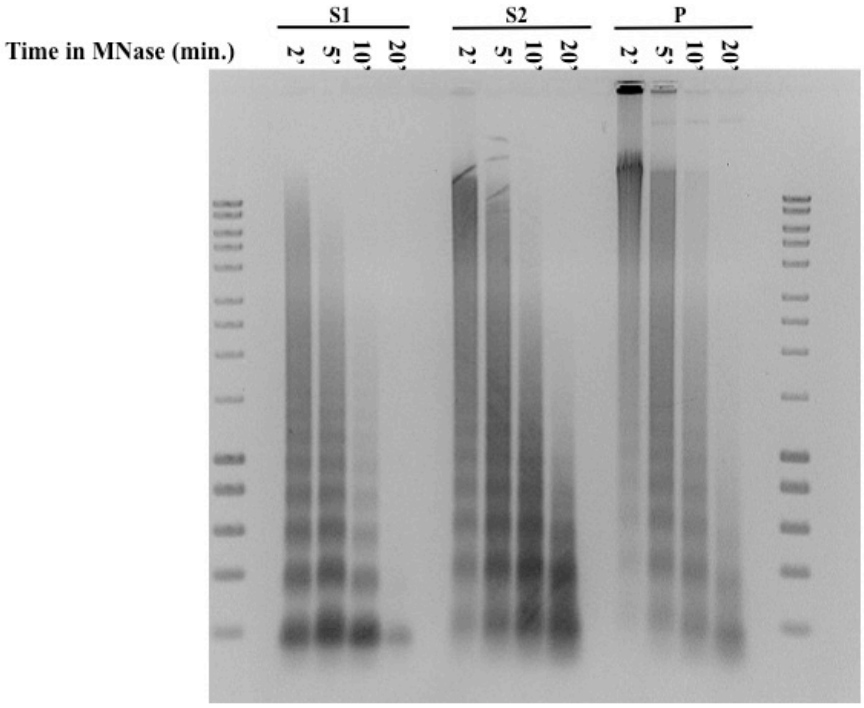

Figure 5. **MNase digestion of chromatin increases with incubation time.** Agarose gel electrophoresis of DNA isolated from multiple time points during MNase digestion of HEK293 chromatin. Supernatant fractions (S1 and S2) and the pellet fraction (P) are shown from left to right in sets of 4 lanes. The 4 time points at which aliquots were taken are denoted above each set of lanes in minutes. Molecular markers to the left and right of the sample lanes denote DNA size in 100 bp steps. Samples were separated on a 1% agarose gel.

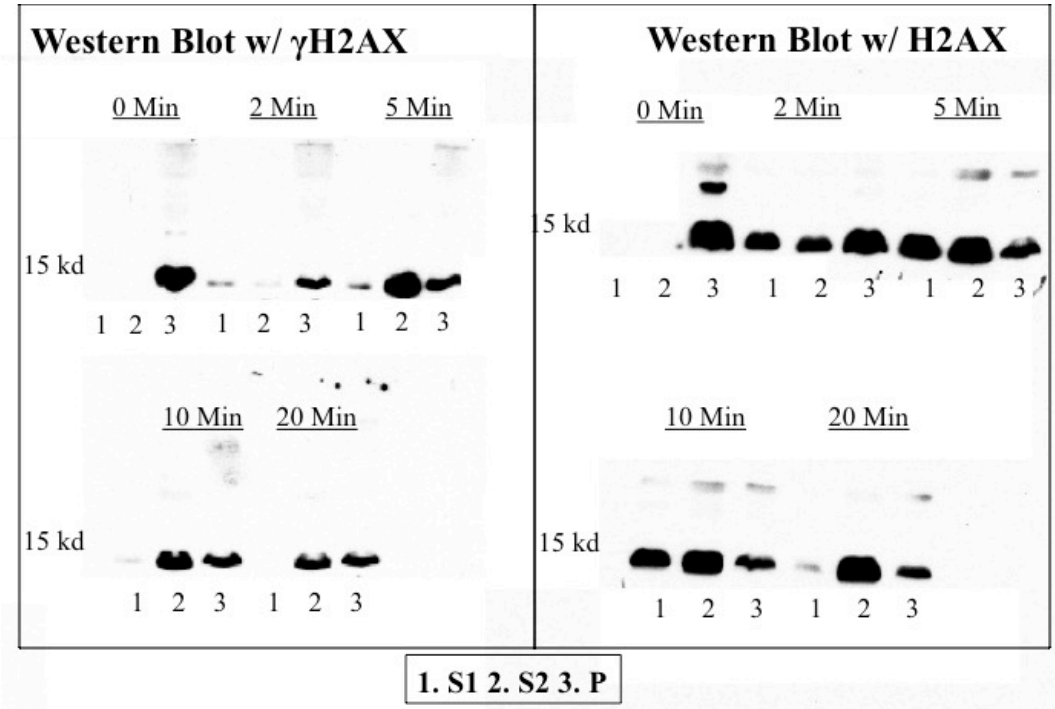

Figure 6. **γH2AX is detected in heterochromatic fractions of the nucleus.** Cell fractionation followed by western analysis of γH2AX and non-phosphorylated H2AX. The left panel shows blotting against γH2AX, and the right panel shows blotting against H2AX. The order in which samples were loaded onto the gel are displayed below the gel and denoted by numbers below each lane. Time points are indicated above each set of lanes in minutes. Molecular weights are shown to the left of each image. Samples were separated using a 15% SDS-PAGE.

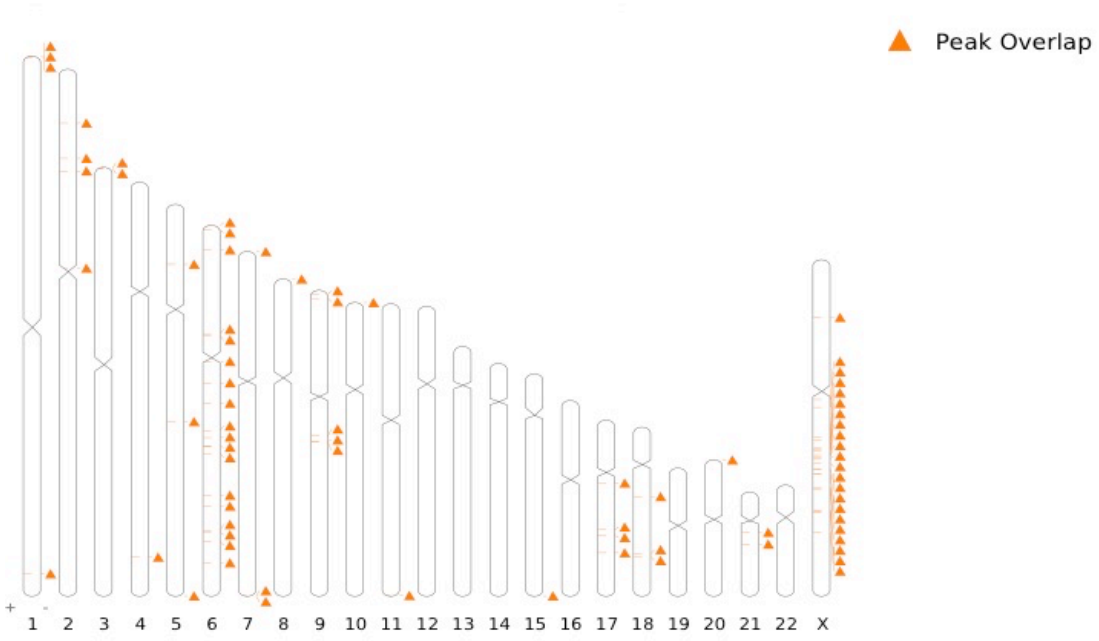

Figure 7. **γH2AX is reproducibly enriched across the human genome in cells that have not been exposed to DNA damaging agents.** ChIP-seq of γH2AX in undamaged HEK293 cells. Mapping data for 23 human chromosomes are listed from left to right. Chromosome number is denoted below each chromosome in the schematic. Orange triangles and their associated bars on the chromosomes denote a threefold enrichment above input in that area of the chromosome. A 200 bp sliding window was used to call peaks. Any peaks found within 600 bps of each other were merged in the analysis. This ChIP-seq experiment is the result of two ChIP samples prepared from two independent groups of crosslinked HEK293 cells.

Chapter 2.1: Introduction: tRNA genes as organizers of the budding yeast nucleus

Large-scale Organization of the Budding Yeast Nucleus

The genome in *S. cerevisiae* provides a simple and elegant system for the study of genome organization. This elegance can be attributed in large part to the small number of genome organizing landmarks that exist in the budding yeast nucleus [48]. The budding yeast genome is composed of 16 chromosomes. In most laboratory experiments, haploid yeast are used. *S. cerevisiae* is able to undergo mitotic divisions in a haploid state [49]. Throughout the budding yeast nucleus, there are several genomic landmarks. One of the first landmarks of note is the nucleolus. Here, the rDNA on chromosome XII organizes in a dense structure that is easily observed with multiple forms of microscopy. In contrast to higher eukaryotes, the budding yeast genome contains only one nucleolus with all of the rDNA repeats. The nucleolus can be found towards one wall of the nuclear envelope [50]. Transcription of both rDNA and some tRNA genes occurs at this structure. Directly across from the nucleolus on the opposite side of the nuclear periphery, the centromeres from each chromosome coalesce around a body embedded in the nuclear membrane called the spindle pole body (SPB). Specialized proteins known as the spindle pole component (SPC) proteins aid in formation of the SPB [51]. The aggregation of the centromeres leads to all of the arms of each chromosome protruding out from the SPB on the nuclear envelope. Telomeres are found at the ends of each chromosome. Telomeres bind silencing proteins and specialized DNA

repair proteins, which in turn aid in clustering telomeres at the nuclear periphery [21]. Interestingly, the telomeres of chromosomes with similar length tend to interact more often with one another than telomeres from chromosomes of different length [35, 48, 52]. Telomeric clusters will also associate with the nuclear periphery and the nucleolus [21, 53-59]. Telomeres, the nucleolus, and the hidden *MAT* (*HM)* loci are the only heterochromatic domains found in the budding yeast genome [1, 60]. It is important to note that while budding yeast centromeres bind canonical centromeric proteins, such as CENPA, budding yeast centromeres are not heterochromatic [61]. The last major landmark that creates constraint on chromosomes is the nuclear envelope. While it is a foregone conclusion that chromosomes can't leave the nucleus, the nuclear envelope plays a critical role in organizing the aforementioned genomic landmarks in the nucleus. These landmarks have been thought of as major organizing centers that aid in organizing the genome in budding yeast. A model for this would predict that landmark interactions create constraint on the chromosomes, which leads to a non-random organization of the genome. A mathematical modeling study done in 2012 tested this model [48]. 5 parameters of constraint in the nucleus were introduced into a computer simulation: 1.) The rDNA is contained in the nucleolus. 2.) The telomeres are at the nuclear envelope. 3.) Centromeric DNA is confined to the spindle pole body. 4.) There are 16 chromosomes. 5.) The chromosomes are confined to the nucleus. Using these parameters, their model was able to predict that chromosomes of similar size tend to interact as a result of volume exclusion that is imposed on chromosome as a result of centromeres being tethered to

the spindle pole body. Volume exclusion could also explain how chromosome arms fell into distinct chromosomal territories. Surprisingly, the chromosome territories that were predicted in the simulation matched up with past studies that mapped territories using DNA FISH. These results have been experimentally and mathematically confirmed in recent studies as well [53, 62]. At the whole genome level, static and long-lasting chromosomal interactions can have profound effects on genome organization. While large scale landmarks in the nucleus have been well characterized, the budding yeast genome also relies on other forces that can have consequences on both genome organization and fidelity.

Genome Organization Occurs through a Network of Long-range Interactions

With the advent of sequencing and genomic interaction techniques, we now have more information at our disposal for studying the genome than ever before. One technique that has given us much insight into the organization of the eukaryotic genome is HiC. By crosslinking chromatin in the nucleus, cutting with a restriction enzyme, and performing a proximity ligation followed by high-throughput sequencing, the Dekker lab was able to show a snap shot of every interaction occurring in a cell [4]. These results corroborated DNA FISH results showing that chromosomes are organized into distinct chromosomal territories in mammalian cells [63, 64]. It also revealed what were called topologically associated domains (TADs). A TAD can be described as a region of the genome that interacts more often with itself than another segment of the genome. A simpler way to imagine this would be that chromosomes organize into a series of loops along the length of the chromosome.

Each loop is physically separated from neighboring chromatin loops. Therefore, each loop can be thought of as a physically separate chromatin domain. TADs display many properties that have led researchers to assign biological function to the creation of these domains. Within a TAD, a distinct TAD is associated with a distinct type of chromatin. For example, DNA within a TAD can display silent chromatin marks, while a neighboring TAD may display active chromatin marks [4, 17]. TADs were originally described as one megabase-wide domains throughout the genome in mammals. However, recent studies have used deeper sequencing and different techniques to improve HiC resolution. Based on those studies, recent estimates show that these domains may be smaller to the tune of ~185 kb [65]. It is important to note that these rules seem to apply to most eukaryotes. Even in organisms that are evolutionarily diverged from mammals, such as *S. pombe*, we find TADs [36]. One of the few eukaryotes where we find an exception to the TAD structure is budding yeast.

In 2010, the Noble lab published a paper in which they presented the first Hi-C done in budding yeast [52]. It revealed a different genomic topology than we find in higher eukaryotes. An overall picture shows that the budding yeast genome displays several characteristics. While there are chromosome territories in budding yeast, there is no evidence for the TAD structure that is observed in mammals. The only portion of the budding yeast genome where we observe TAD-like interaction behavior is the rDNA locus on chromosome 12. At the rDNA locus, regions of the chromosome along the rDNA repeats interact to form the nucleolus. A recent study

of a native and synthetic budding yeast chromosome 12 has shown that the presence of the rDNA interaction splits the arms of chromosome 12 into two non-interacting domains. Interestingly, if the rDNA repeats are moved to a different chromosome, the same conformation is assumed [66]. Aside from the nucleolus, TADs are not found in the budding yeast genome. Corroborating previous DNA-FISH and immunofluorescence data, Hi-C data show increased interaction between centromeres of each chromosome throughout the genome [67]. The Hi-C data also show that those inter-chromosomal interactions tend to occur between chromosomes of similar size. However, inter-chromosomal interactions are much less frequent than intra-chromosomal interactions.

Proteins That Mediate Long-Range Interactions in Budding Yeast

Structural maintenance of chromosome (SMC) proteins play a critical role in mediating chromosomal interactions across all eukaryotes. These proteins are necessary for the survival and propagation of budding yeast. This is evidenced by that fact that null mutants in any of the SMC proteins, or the associated loading complex, are not viable [68]. In budding yeast, the main SMC proteins are cohesin and condensin. Both of these protein complexes are deposited on chromosomes in an SCC2 dependent manner [69-73]. For this reason, SCC2 has been called the SMC protein loading complex. The literature on SMC proteins is immense. These proteins have been heavily studied since their discovery in a variety of contexts including: chromosome segregation, heterochromatic interaction, DNA repair, gene expression,

etc. [74-76]. This review will focus on current literature that reveals the role of SMC proteins in organizing the genome.

Cohesin is a ring-like protein complex composed of several subunits. SMC1 and SMC3 form a dimer that creates the ring-like structure of the cohesin protein. This protein dimer complexes with a protein called Mcd1 (aka Scc1), and Mcd1 acts as a clamp to hold the ring structure closed. Cohesin deposition displays several characteristics across chromosomes in budding yeast. We see a distinct enrichment of cohesin at the pericentric region of all chromosomes [68, 73, 77]. This enrichment facilitates proper biorientation of chromosomes during mitosis and meiosis by having a pool of cohesin available to establish sister chromatid cohesion [75]. Cohesin is also enriched in a semi-periodic pattern along chromosome arms, showing preference for AT rich regions that have been appropriately named cohesin-associated regions (CARs). Cohesin shows a preferential enrichment at intergenic regions between transcribed convergent genes [73]. This has led researchers to propose a variety of models on how cohesin associates with chromosomes and what leads to its enrichment at intergenic regions. A popular model is that the cohesin ring actually slides along the chromosome with an actively transcribing polymerase, and this leads to the deposition of cohesin at convergent intergenic regions [71]. At a genome-wide level, cohesin enrichment also occurs at repressed regions. Segments of the genome with active transcription tend to be weakly associated with cohesin. One way to interpret this result is that actively transcribed regions favor cohesin disassembly, and repressed regions favor cohesin assembly [77]. The data seem to support both the

sliding and assembly/disassembly models. Therefore, it is very likely that there is a combination of both models working to achieve the cohesin distribution we observe. Budding yeast cells can be starved of amino acids to induce the biosynthetic amino acid synthesis pathway. Interestingly, starvation induced genes that show an enrichment of cohesin before starvation, show a significant decrease in cohesin occupancy upon transcriptional activation. The decreased cohesin occupancy at induced genes is accompanied, in some cases, by an appearance of a downstream cohesin peak. This suggests that at a repressed region, enriched for cohesin, cohesin is lost in the area upon transcriptional activation. The appearance of the downstream cohesin peak suggests that cohesin could have been redistributed with transcription. This result is suggestive of cohesin sliding. In contrast to this scenario, the same study found that there are genes that are transcriptionally induced by starvation; those genes display a depletion of cohesin from promoter regions, but show no new cohesin peak downstream of the gene. Taken together, these results support a model for cohesin sliding and cohesin disassembly in response to active transcription.

Sister chromatid cohesion is important for ensuring biorientation of chromosomes for proper segregation [75, 78]. For this reason, elements that are thought to have a role in this process have been extensively studied in the budding yeast genome. Classical assays to determine levels of sister chromatid cohesion are done by incorporating a fluorescent reporter at a locus of interest along a chromosome arm [76, 79]. In most cases this is done with an array, for example lacO, which is used to recruit a fluorescent fusion protein, i.e. lacI-GFP. The idea

behind this assay is that after S-phase two separate arrays exist in the cell. The cells can then be arrested in metaphase and visualized with fluorescent microscopy. Proper cohesion is signified by both arrays being condensed into one focus, and a defect in cohesion is identified as a separation of the arrays or the appearance of 2 fluorescent dots. The Gartenberg lab has taken great advantage of this assay to make many important observations on how cohesion is established and maintained [76, 79]. Prior to a 2007 study, it was known that *HMR* loads cohesin proteins. The Gartenberg lab had also found that when excised as an extra-chromosomal circle, *HMR* is able to maintain cohesion as shown by the classical cohesion assay. The recruitment or maintenance of the cohesin found in this region was dependent on the SIR histone deacetylase complex [79]. However, it wasn't clear just how cohesion was established at this locus. In 2007, a reductive approach was taken to examine just what cis-elements aided in establishing cohesion of excised *HMR* circles. Dubey and colleagues showed that the tDNA just outside of *HMR* is necessary for deposition of cohesin at HMR during S-phase of the cell cycle. This deposition was also dependent on SIR proteins. Taken together, these results provide evidence to show that tDNAs are important in establishing cohesion in the budding yeast genome.

The other prominent SMC protein throughout the genome is condensin. Condensin has a very similar structure to that of cohesin. However, the two proteins that make up the dimer that will form the ring of condensin are SMC2 and SMC4 [80, 81]. The clasping molecule that holds the ring structure closed is Brn1. Condensin shows a similar distribution to cohesin across the chromosome with many sites

distributed across the chromosome. The strongest sites of enrichment tend to be origins of replication and the pericentric region [69]. However, there are also peaks of condensin, and Scc2, at tDNAs across the genome. Upon deletion of tDNA elements, it was found that both condensin and RNA Pol III transcription factor TFIIIC occupancy were reduced at loci where tDNAs were deleted. Importantly, TFIIIC and condensin loading were not abolished after tDNA deletion. This tells us that while the cis elements contained in the tDNA sequence (i.e. b-box sequence) are important to condensin recruitment, other cis-elements may also contribute. Work from our lab has been able to show that all tDNAs are not created equal at carrying out functions in the genome. For example, the replacement of a tDNA outside of the cryptic mating locus *HMR* with another tDNA is able to compensate for the barrier activity of the native tDNA. However, it is evident that the spread of the silent chromatin at HMR is not stopped as effectively upon replacement [82, 83]. Therefore, there are elements in the flanks of tDNA elements that have important consequences on the ability of these tDNAs to recruit proteins to the locus. Currently, this is an open question in the field and further work is necessary in order to elucidate exactly what cis elements may aid in recruitment of SMC proteins along with tDNAs.

Mitotic Genome Organization in Budding Yeast

Another observation that has been made about the organization of tDNAs throughout the genome is that they tend to cluster towards the nuclear periphery and nucleolus [55, 84]. This was first observed by fluorescent microscopy [85, 86].

Several years ago our lab sought to characterize the mechanism by which peripheral localization of tDNAs occurs. We focused on the tDNA insulator element just outside of *HMR* on chromosome III. We first showed, through zone analysis, that nuclear pore proteins (NUPs) play an important role in localizing this tDNA to the periphery. Furthermore, NUP proteins physically interact with the tDNA, and ectopic NUP recruitment is sufficient to induce peripheral localization of a non-peripheral locus [55]. Further investigating this phenomenon, the Gartenberg lab was able to show that peripheral localization of tDNAs was not unique to the *HMR* tDNA. Gartenberg's lab found that tDNA peripheral localization is a general feature that occurs at all phases of the cell cycle. Additionally, higher levels of peripheral localization were observed during the mitotic phase of the cell cycle [84]. Peripheral tDNA localization was dependent on NUP recruitment to tDNAs along with cohesin loading throughout the cell cycle. Increased transcription at tDNAs and binding of the los1 protein was also shown to be important to the increased peripheral localization during mitosis. It has been proposed that this increased localization at the nuclear pore could be related to "gating" through which transcription is tied to the NUP complex to facilitate faster transport of important transcripts, such as tRNAs. However, further work is necessary to fully elucidate the importance of this process.

Open Areas of Study on Genome Organization in S. cerevisiae

Organization in budding yeast has been studied extensively. However, a large amount of mechanistic experimentation needs to be done. There are many open questions on what mechanisms are responsible for basic genomic architecture. For

example, how important are tDNAs to overall genomic organization and fidelity? tDNAs can exert a large influence as cis-elements in the genome through their ability to separate chromatin domains and recruit SMC proteins. However, the importance of tDNAs as drivers of global genomic architecture is still not fully understood.

Chapter 2.2: Transfer RNA Genes Affect Chromosome Architecture and Function

Omar Hamdani[1], Tsung-Han S. Hsieh[3], Takahiro Fujita[4], Josefina Ocampo[5], Jacob G. Kirkland[1], Josh Lawrimore[6], Tetsuya J. Kobayashi[4], Brandon Friedman[6], Derek Fulton[6], Masaya Oki[4], Kerry Bloom[6], David J Clark[5], Oliver J. Rando[3], Rohinton T. Kamakaka[1,2]

1 Department of MCD Biology**,** 1156 High Street, University of California, Santa Cruz, CA 95064 USA
E-mail: rohinton@ucsc.edu

2 Corresponding Author

3 Department of Biochemistry and Molecular Pharmacology, University of Massachusetts Medical School, Worcester, MA 01605, USA
4 Department of Applied Chemistry Biotechnology, University of Fukui, Bunkyo, Fukui, Japan.
5 National Institutes of Health, 6 Center Drive, Bethesda MD 20892 USA
6 Department of Biology, University of North Carolina at Chapel Hill, Chapel Hill, NC 27599-3280 USA

Abstract

Chromosomes are packaged and organized in the nucleus in an ordered, non-random manner. This organization influences many nuclear processes such as transcription, gene silencing and mitosis. While transfer RNA genes (tDNAs) are essential for the generation of tRNAs, these gene loci are also binding sites for transcription factors and chromosomal architectural proteins.

In the yeast *Saccharomyces cerevisiae*, tDNAs are dispersed along all sixteen chromosomes. In this study, we investigated the role of tDNAs in genomic organization and nuclear function by editing a chromosome so that it lacks any tDNAs. Our analyses of this tDNA-less chromosome shows that loss of tDNAs affect nucleosome positioning, binding of SMC proteins, centromere clustering, long-range chromosome folding and epigenetic gene silencing. We propose that these effects are primarily mediated via changes in local interactions between tDNAs and other regulatory sequences. These changes then manifest as alterations in long-range chromosome architecture with effects on gene regulation over large distances.

Introduction

The three dimensional organization of the yeast nucleus is non-random (Reviewed in [87, 88]). Each chromosome occupies a specific territory in the nucleus anchored to nuclear substructures via specific DNA sequences. The telomeres of each chromosome tend to associate with one another and with the nuclear envelope in small clusters, based on the length of the chromosome arms. The sub-telomeric

heterochromatic loci reside at the nuclear periphery, though they are excluded from the nuclear pores [55, 89, 90]. The rDNA repeats on chromosome XII are packaged into a dense structure, known as the nucleolus, at the nuclear periphery [50]. Opposite the nucleolus is the spindle pole body, which is the interphase attachment site for the centromeres of the 16 chromosomes [51]. The active genes along the chromosome arms primarily reside in the nuclear interior with some active genes residing at nuclear pores [48, 52, 87].

Besides DNA sequence elements, numerous proteins play a role in this organization via networks of interactions between nuclear membrane proteins and proteins bound to chromatin. Chromatin bound proteins involved in this organization include heterochromatin proteins [56], lamin like proteins [57, 58, 91-93], specific transcription factors [94, 95], RNA polymerases [50] and DNA repair proteins [1, 18] (see [87] for review).

tRNA genes (tDNAs) are a class of active genes found on all chromosomes, and are bound by transcription factors and RNA polymerase III. tDNAs are short, highly transcribed DNA sequences [96] that are usually nucleosome free with strongly positioned flanking nucleosomes [97-100]. The tDNAs contain internal promoter elements called A and B-boxes, which aid in the binding of transcription factor TFIIIB and TFIIIC [101, 102]. Transcription factor binding and nucleosome eviction is mediated by the chromatin remodeler RSC, which localizes to tDNAs [83, 103, 104]. While many individual tDNAs are prone to mutational inactivation and gene loss [105-107], a subset is syntenic with respect to neighboring sequences [44, 108].

Data suggest that these conserved tDNAs possess position-specific functions in gene regulation (reviewed in [109, 110]). For example, tDNAs have been shown to function as heterochromatic barrier insulators, which stop the spread of heterochomatic domains into adjacent non-silenced domains [44, 82, 83, 111]. Additionally tDNAs regulate RNA pol II transcribed gene expression in yeast, *Drosophila*, mouse and human cells by acting as enhancer blockers [17, 44, 112-116].

In many organisms, tDNAs have been shown to cluster at a few specific sites in the nucleus [44, 110, 117, 118]. In *S. cerevisiae*, RNA FISH and genomic studies have shown that a third of the tDNAs cluster together on the outer periphery of the nucleolus [85], while another third cluster adjacent to centromeres [52]. In the distantly related fission yeast, *S. pombe*, tDNAs also cluster together adjacent to the centromere [119, 120]. Immunofluorescence and genomic 4C/HiC analysis demonstrate tDNA clustering in other eukaryotes as well [17, 44, 65, 117, 121, 122].

tDNA-bound transcription factors provide auxiliary functions via their interactions with other nuclear cofactors including chromatin remodelers, histone modifiers, nuclear pore proteins and chromosomal architectural SMC proteins. Studies from several labs have shown that tDNAs are associated with the cohesin (Smc1/Smc3) [73], and condensin (Smc2/Smc4) complexes [69, 86], as well as the SMC loading proteins (Scc2/Scc4) [72, 123]. The loading of the SMC proteins onto tDNA sequences is dependent on the tDNA promoter and the RSC remodeler [69, 77, 124].

The clustering of tDNAs at specific sites in the nucleus suggests that tDNAs likely play a role in chromosome packaging and nuclear organization. To challenge this model, we generated a "tDNA-less" chromosome through the systematic deletion of all the tDNAs on chromosome III in *S. cerevisiae*. We characterized the chromatin packaging and nuclear localization of this chromosome. Our results show that tDNA loss affects nucleosome positioning, chromosome mobility, and chromosome architecture. These alterations have surprising functional consequences for diverse nuclear processes, including meiotic cross over frequencies, centromere clustering and the stable inheritance of gene silencing.

Results

The 275 tDNAs in the budding yeast genome are dispersed across all 16 chromosomes. Chromosome III is 316 kb long and has 10 tDNAs spread across both arms of the chromosome. In order to investigate the role of tDNAs in chromosome organization and function, we have created a strain in which chromosome III is devoid of any functional tDNAs by deleting a small fragment of each tDNA containing the internal promoter elements. For simplicity, we have labeled the tDNA adjacent to the *HMR* locus as t0 and have labeled the remaining nine tDNAs going from right to left as t1, t2, t3 etc (Figure 1).

In the wild type yeast strain W-303, both tDNAs t3 (*tK(CUU)c*) and t4 (*tM(CAU)c*) are naturally missing along with genomic sequences located between these two tDNAs. To delete the remaining eight tDNAs we first replaced the segment between the tDNA promoter A and B boxes with the *URA3* gene, and then

subsequently replaced *URA3* with a DNA fragment containing a unique DNA barcode. This involved multiple sequential transformations. Each deletion was monitored by PCR analysis, and intermediate strains were backcrossed to wild type W303 prior to additional rounds of transformations. tDNA t1 (*tS(CGA)c*) is essential in *S. cerevisiae* [125] and there are only two copies of tDNA t7 (*tP(AGG)c*) in the genome such that loss of t7 caused cells to grow more slowly. In order to remove these two genes from chromosome III and simultaneously maintain the health of the yeast, we integrated single copies of these two genes on chromosome XV at the *HIS3* locus. There are between 10 and 16 copies of the other tDNAs, and so removal of one of these should not have effects on cell growth due to tRNA biosynthesis or translation efficiency. Once the full tDNA delete chromosome had been constructed, the strain harboring this chromosome was backcrossed with wild-type W-303, and segregation of the deleted tDNAs was monitored by PCR using primers specific to the unique barcodes.

The tDNA delete strain did not show any gross growth defect, forming homogeneous and healthy looking colonies. Strains bearing this tDNA-less chromosome had a doubling time of ~90 minutes which was indistinguishable from a wild type W-303 strain. Qualitative chromosome loss assays in a homozygous diploid strain, based on the appearance of pseudohaploids capable of mating, showed no defect in chromosome loss rates indicating that the mitotic cell cycle had not been perturbed (data not shown).

Nucleosome positions are specifically altered surrounding the tDNAs

tDNAs are bound by the transcription factors TFIIIC and TFIIIB and are highly transcribed. The stable binding of transcription factors as well as their interactions with chromatin remodelers and SMC proteins results in nucleosome eviction at the gene and positioned nucleosomes flanking the genes. We therefore turned our attention to how loss of tDNAs changes the basic chromatin organization along chromosome III. Well-defined nucleosomes and highly transcribed genes can have an effect beyond just the local area where they lie on the chromosome [77]. In order to determine if tDNAs affect nucleosome positions across chromosome III, we mapped nucleosomes in our tDNA delete strain as well as in the wild type strain.

Haploid yeast cells were grown to log phase, harvested and digested with varying concentrations of micrococcal nuclease to generate mono-nucleosomal size DNA fragments, which were subjected to paired-end MNase-seq. Analysis of the nucleosome mapping data show that nucleosome positions on all of the chromosomes except chromosome III remained the same in both the wild type and the tDNA delete strains (data not shown). Consistent with this data, nucleosome positions around tDNAs on these chromosomes were also unchanged. Analysis of the 265 tDNAs on all chromosomes except chromosome III revealed no change in nucleosome positioning at these tDNA sites (Figure 2A).

In contrast, changes in nucleosome occupancy were observed at or immediately adjacent to the mutated tDNAs on chromosome III (Figure 2B). Figure 2B shows the average nucleosome occupancy across 2kb segments centered on chromosome III tDNAs. Each tDNA in WT cells is aligned at its 5' end, while tDNAs in the delete

strain are aligned at the 5' end of the deletion point. In the wild type strain, there is a clear nucleosome free region centered on the tDNA flanked by positioned nucleosomes. In the strain where the tDNA promoters have been deleted, this pattern is altered and nucleosomes populate the entire segment. Nucleosome positions elsewhere on chromosome III that are distant from the tDNAs are not altered on the tDNA-less chromosome (data not shown). These results indicate that tDNAs create nucleosome free regions at tRNA genes with positioned nucleosomes flanking the gene, but their chromatin organizing effects are locally confined and do not extend beyond their immediate vicinity.

SMC protein binding at tDNAs is dependent upon a functional tDNA

The SMC proteins play a pivotal role in higher order chromosome structure and function. Since many tDNAs are sites for the recruitment of these proteins, we asked if loss of all the tDNAs on chromosome III reduced recruitment of these proteins at these loci. We first mapped the binding of the SMC protein loader Scc2 at chromosome III tDNAs via ChIP-qPCR against Myc-tagged Scc2 (Figure 3). A site at the *OCA4* gene was used as an internal control since this site does not bind Scc2 in wild type cells. We were unable to design unique primers at t6 due to the presence of repetitive sequences in the immediate vicinity of this gene and therefore could not map the localization of these proteins at this tDNA. In wild type cells, Scc2 is enriched at four of the tDNAs present on chromosome III, though it is largely absent from three tDNAs (t1, t7 and t9). We observed a ~3.5 fold enrichment at t8 and a ~2.5 enrichment at t0, t2 and t5. When the same protein was mapped in the strain lacking

functional tDNAs on chromosome III, we observed a significant reduction in Scc2 binding at all the tDNAs that were enriched in WT. The levels dropped to those observed for the negative control *OCA4* except for the t8 tDNA, where the level dropped two fold but there was some residual Scc2 still present (Figure 3B). The amount of Scc2 did not change at *CEN3* when the tDNAs were absent from the chromosome, indicating that the binding of Scc2 to the centromere was independent of the tDNAs. These data show that some tDNAs are sites of enrichment for Scc2 on chromosome arms, and deletions of the internal tDNA promoters reduced enrichment of Scc2 at these sites.

Scc2, in association with Scc4 helps recruit the SMC condensin complex to chromatin. Condensins localize to tDNAs, and are necessary for the clustering of tDNAs in the nucleus [69, 86]. We therefore mapped the binding of condensins at tDNAs on chromosome III using the HA-tagged Brn1 subunit. The data in figure 3C show that in wild type cells, the Brn1 profile was very similar to that previously observed for Scc2 with significant binding of Brn1 at specific tDNAs. Correspondingly, the binding of the condensins was significantly reduced at these sites upon deletion of the tDNA promoters.

Specific loci on the right arm become more mobile in the tDNA-less chromosome

tDNAs are described as chromosome organizing clamps because of their consistent association with certain landmarks within the nucleus, the centromere and the nucleolus [52, 85, 119]. We therefore aimed to assess whether the tDNAs on

chromosome III play any role in tethering this chromosome to nuclear sub-structures. We tested the prediction that loss of nuclear tethering should result in altered chromosome III mobility within the nucleus. To test this, we performed mean squared distance analysis (MSD) on chromosome III in wild type and the tDNA delete strains. In this assay, the location of a point on the chromosome is mapped in 3D space over a defined period of time in relation to a fixed point within the nucleus [126-128]. The fixed point we used for this assay was the spindle pole body (marked with an Spc29-RFP fusion protein). Eight chromosomal loci across chromosome III were assayed (Figure 4). These loci were tagged by inserting LacO arrays at these sites, and monitoring the movement of LacI-GFP fusion protein mediated fluorescence. Time-lapse movies of individual cells were imaged over the course of 10 minutes. Z-stack images of the cells were taken every 30 seconds during the time-lapse, and MSD was calculated at each time-point using the following equation: $<(X_t - X_{t+\Delta t})^2>$. Using this information, MSD curves were generated for each locus in both the WT and tDNA delete strain (Supplementary Figure 1). The plateau of the MSD curve was used to calculate the radius of constraint (Rc) for each locus. Each locus that was assayed is shown on the x-axis, and its Rc value is plotted as a box plot on the y-axis in nm. For the wild type chromosome III, *CEN3* was most constrained (Rc=415 nm), with loci located further from the centromere exhibiting greater mobility. For example, *LEU2*, which is approximately 30kb from the centromere, had an Rc of 522nm while *HMR*, which is approximately 180kb from the centromere, had an Rc value of 688nm. This is consistent with previous data showing that the location of a locus in relation to the

centromere is critical in determining mobility, with loci closer to the centromere displaying decreased mobility compared to loci farther from the centromere [48, 53].

Out of the eight loci assayed, the *MAT* and *BUD31* loci showed a statistically significant change in mobility following the loss of tDNAs, with both loci showing a higher Rc compared to the WT strain (Figure 4). At the *MAT* locus, the Rc increased from 587 nm in WT to 713 nm after tDNA deletion. At *BUD31*, the Rc increased from 505 nm in WT to 632 nm after tDNA deletion. At the other six loci that were assayed, there were no significant differences in Rc upon the deletion of tDNAs. These results suggest that some tDNAs participate in constraining chromosome segment motion.

Centromere clustering is increased upon loss of tDNAs

SMC proteins localize to tDNAs. Since SMC proteins play a central role in long-range chromatin interactions and nuclear architecture, tDNA-mediated SMC loading could potentially drive chromosome folding as well as chromosome organization in the nucleus. In order to test this, we set out to determine the detailed three-dimensional organization of a chromosome III lacking functional tDNAs. To address this question we used a modified chromosome conformation capture technique called Micro-C [35, 129]. In brief, yeast cells were first crosslinked with formaldehyde and DSG, followed by micrococcal nuclease digestion to fragment chromatin into mononucleosomes. Crosslinked, digested chromatin was then ligated to capture chromosomal interactions. Following ligation, the chromatin was size selected and subjected to paired-end high-throughput sequencing. The sequencing reads were

mapped back to the reference genome to determine which regions of the chromosome were interacting with other regions. Comparison of Micro-C maps for wild type and tDNA mutant strains revealed no dramatic differences in overall chromosome architecture between the tDNA delete and wild type strains. As previously described, ~2-10 kb contact domains encompassing ~1-5 genes were observed across all 16 chromosomes in both the wild type and tDNA-less strain. Analysis of chromosome III in wild type and tDNA delete cells showed that these domains persisted even upon loss of the tDNAs (Supplemental Figure 2). Thus, tDNAs are not responsible for the general packaging of the chromosome fiber.

While the overall folding of chromosome III was not altered in the absence of tDNAs, we did identify a number of changes at specific loci. Most notably, we observed substantial changes in the behavior of the centromere on chromosome III (Figure 5A). The 16 centromeres in yeast are in close proximity with one another, and cluster adjacent to the spindle pole body [51, 67, 130]. These CEN-CEN interactions can be captured by both HiC and Micro-C crosslink analysis [52, 63], and are recapitulated in this study in the W303 strain background. Interestingly compared to the wild type strain, the centromere of chromosome III in the tDNA delete strain showed an increased frequency of interactions with the other centromeres. Focusing on the 50kb pericentric region of each chromosome, we found that most CEN-CEN interactions were unaltered in the tDNA deletion strain. For instance, focusing on interactions between the chromosome XVI centromere and the remaining centromeres showed that interactions between *CEN16* and the majority of

centromeres remained unchanged, but that there was a ~20% increase in interaction strength between *CEN16* and *CEN3* when chromosome III lacked tDNAs.

This increase in *CEN3* interaction was not confined to *CEN16*. When the same analysis was performed using *CEN3* as an anchor, we observed increased frequency of interactions between *CEN3* and all of the other chromosomal centromeres when chromosome III lacked tDNAs. Most of the interaction counts increased approximately 20% compared to WT, with the highest increase seen at C*EN3-CEN9*. These results demonstrate that upon deletion of all tDNAs across chromosome III, inter-chromosomal interactions increase between *CEN3* and the other centromeres.

tDNAs play a role in *HML-HMR* long-range association

The silent loci *HML* and *HMR* reside on chromosome III, separated by approximately 300kb along the linear chromosome. However, the *HML* locus, located 11kb from *TEL3L*, is in close 3D proximity to the *HMR* locus, located 23kb from *TEL3R*. This long-range interaction has previously been detected both microscopically as well as by HiC analysis [1, 63, 131]. We recapitulate this finding in the Micro-C experiment with the wild type strain. Comparing wild type cells to the tDNA delete strain, we noticed that the interaction of *HML* with *HMR* was altered in the tDNA delete strain (Figure 5B). In wild type cells, there was a significant interaction between *HML* and *HMR* and this interaction zone became less defined and more diffuse upon deletion of the tDNAs from chromosome III. Rather than being restricted to a limited region surrounding the loci, increased interaction frequency was observed across a broader region of chromosome III. While *HMR* still interacts with

HML in the deletion strain, *HMR* appeared to also display increased interactions with *TEL3L* suggesting that its interaction frequency with *HML* has likely changed. Similarly, the segment containing *HML* showed increased interactions with *TEL3R* (rather than being restricted to interacting with sequences at *HMR)*. These results suggest that deletion of chromosome III tDNAs perturbed long-range interactions between the two silent mating type loci on this chromosome.

As the t0 tDNA immediately adjacent to *HMR* has been shown to function as an insulator [82, 132], we wished to determine if this specific tDNA influenced *HML-HMR* interactions. We generated a strain with 256 copies of the Lac operator inserted adjacent to *HMR* and 116 copies of the Tet operator inserted adjacent to *HML*. Expression of the fusion proteins CFP-LacI and YFP-TetR in this strain enabled us to visualize these loci in living yeast by fluorescence imaging. The distance between *HML* and *HMR* was then measured in wild type and a strain lacking the t0 tDNA. We found that in wild type cells, *HML* was in close proximity to *HMR* and the median distance between these loci was around 450nm. Consistent with our expectations, deletion of Sir proteins resulted in separation of these loci, with the median distance increasing to around 800 nm. Importantly, when we eliminated the tDNA, this led to an increase in the distance between *HML* and *HMR* compared to wild type cells. The median distance between *HML* and *HMR*, upon deletion of t0, shifted to ~700 nm (Figure 5C), indicating that there was a perturbation of the *HML-HMR* interaction.

tDNA presence increases epigenetic gene silencing

Since tDNAs affected the long-range association between *HML* and *HMR*, we next asked whether this affected gene silencing at these loci. Silencing can be assayed by insertion of fluorescent reporter genes placed immediately adjacent to *HML* and *HMR*. These reporter genes are metastably silenced in wild type yeast. We decided to investigate gene silencing in various strains containing or lacking tDNAs on chromosome III.

A cassette containing an H2B (*HTB1*) promoter driving *HTB1-EYFP* was integrated to the right of *HML* while a cassette containing the *HTB1* promoter driving *HTB1-ECFP* was integrated to the left of *HMR*. In addition, on chromosome XV, a cassette containing an *HTB1* promoter driving *HTB1*-mCherry was integrated as a control euchromatic marker [133]. The H2B-mCherry gene is active in all cells in the population. The *HML::YFP* and the *HMR::CFP* reporter genes are present immediately outside of *HML* and *HMR* but reside in a region bound by Sir proteins [55, 97]. These genes adopt one of two expression states, either active or silent. For visualization, single cells were placed on microfluidic plates and monitored continuously by fluorescence microscopy. Fluorescent signal from each individual cell was recorded every 40 minutes over a period of ~24 hours. This allowed us to trace the lineage of each daughter from the founder cell, and score the cells according to the expression of the reporter genes at *HML* and *HMR*. Cell lineage trees were traced, and each cell in the lineage was assigned a positive or negative value for expressing each reporter as it underwent cell division (Figure 6A).

We initially analyzed the silencing of the reporter genes in the wild type strain. Consistent with previous data [133], reporters at *HML* and *HMR* were regulated such that the reporters maintained their activity state over many generations. Only occasionally, reporter genes switched to the opposite expression state. Once they switched they maintained the new state for several generations. Furthermore, when one reporter was active the other was also more likely to be active, though this coordination is not an absolute effect.

We next investigated silencing of the reporters in a strain where chromosome III lacked all the tDNAs. In this strain, the reporters at *HML* and *HMR* were active more often compared to the wild type strain. Furthermore, the silenced state was less stable, and switched to the active state more rapidly. These effects were observed at both *HMR* and *HML* even though there are no tDNAs adjacent to *HML*.

While expression states at both *HML* and *HMR* were more often than not stably inherited, the transcriptional state did flip in some daughter cells (Figure 6B). An expressed to repressed transition was a less frequent event compared to the repressed to expressed transitions regardless of genotype. This is not entirely surprising since the reporter genes were inserted immediately outside of the two silencers in a zone where the silent state is metastable [134, 135]. When analyzing the repressed to expressed transitions, we saw a discernible difference in the frequency of the expression of the reporter genes at both *HML* and *HMR*. The full tDNA delete strain showed an increased frequency of cells undergoing the transitions at both *HML* and *HMR* compared to wild type cells.

Transcriptional states of the reporters were affected at both *HML* and *HMR* in a strain containing full tDNA deletions on chromosome III, even though only *HMR* has a tDNA adjacent to it. Given this information, we decided to focus on the tDNA (t0) that resides immediately adjacent to *HMR* and functions as an insulator at *HMR*. This allowed us to address whether the specific t0 tDNA is necessary and/or sufficient for the changes in transcriptional regulation adjacent to the *HML* and *HMR* loci. To test whether t0 is necessary for regulating silencing states, we built a strain where chromosome III contained all of the tDNAs except t0, which was deleted (-t0). The lineage tree showed that this strain behaved similarly to the strain lacking all tDNAs, such that both reporters were active most of the time and rarely switched to the repressed state. Like the full tDNA delete, the -t0 strain showed an increased frequency of cells undergoing the transitions at both *HML* and *HMR* when compared to the wild type strain, where a reporter gene that was not expressed in one generation was more likely to be expressed in the next generation.

Alternatively, to determine if the t0 tDNA was sufficient for mediating silencing effects at *HML* and *HMR*, we constructed a strain lacking all tDNAs except for t0, still being present adjacent to *HMR* (+t0). Again, we monitored expression of the reporters at *HML* and *HMR* in this background. The lineage tree showed that this strain behaved similarly to the wild type strain, such that both reporters were silent more often than the full tDNA delete and -t0 strains. Wild type and +t0 strains also inherited the silent state with greater fidelity.

Taken together, the data suggest that deletion of tDNAs on chromosome III had an effect on the ability of *HML* and *HMR* to modulate the expression state of a reporter gene placed near either locus. More specifically, t0 may be the tDNA primarily responsible for the phenotypes. Data from -t0 and +t0 strains suggest that this single tDNA adjacent to *HMR* is both necessary and sufficient to drive the expression state of the reporters at both *HML* and *HMR*.

Discussion

tDNAs are middle repetitive DNA sequences scattered across all 16 chromosomes. Their primary function is the synthesis of tRNAs. In this manuscript, we show that tDNAs are also mediators of chromosome architecture. They 1) help tether segments of chromosomes, restricting the mobility of these segments, 2) affect nuclear architecture by influencing centromere and heterochromatin clustering, and 3) alter the fidelity of the inheritance of gene silencing. These effects are unlikely to be due to reduction in copy number of the tDNAs since all of the tDNAs (except t1 and t7) have between 10 and 16 copies in the cell, and all of these copies are transcriptionally active [136-138].

tDNAs locally affect nucleosome positioning

The binding of specific proteins to a site on the DNA can affect nucleosome positions over long distances [139]. However, for tDNA bound transcription factors TFIIIC and TFIIIB [83, 97, 99, 100, 136-138, 140, 141], the effects are local and not transmitted over long distances. Nucleosome depletion at the gene start site and positioned nucleosomes flanking the gene are a hallmark of tDNAs. Our data show

that mutations in tDNA promoters only affect nucleosome positions in the immediate vicinity of the tDNA. These data indicate that the presence of stably bound TFIIIC and TFIIIB function via steric mechanisms to statistically position nucleosomes [142] in the vicinity of the tDNA, but this effect does not get transmitted along the chromosome.

tDNAs and SMC proteins

tDNAs are nucleosome-free sites where the transcription factors TFIIIC and TFIIIB recruit the chromatin remodeler RSC [72, 83, 103, 104] and the SMC proteins [124, 143]. The SMC proteins are involved in higher order chromosome organization in all eukaryotes and have been extensively mapped. tDNAs are binding sites for all three classes of SMC proteins (cohesins, condensins and repairsins), the SMC protein loader Scc2/4, and the meiotic Rec8 SMC protein [69, 73, 123, 144-147]. Furthermore, γ-H2A is enriched near tDNAs [2, 148], and plays an important role in the binding/stabilization of the SMC proteins [1, 146]. Given these intimate connections between tDNAs and the SMC proteins, we investigated the effects of SMC protein loading upon tDNA deletion from the chromosome. Our data indicate that loss of the tDNA promoters does lead to loss of SMC proteins from tDNAs. This effect is tDNA specific since we do not see a loss of SMC proteins from centromeres.

However, this loss of SMC proteins does not translate into dramatic alterations in chromosome behavior with cohesion alterations at one site and no discernible effects on chromosome loss rates (data not shown). This is most likely due to redundancy because while approximately half of the tDNAs are bound by SMC proteins, only a

third of the SMC protein binding sites localize at or near tDNAs [69]. The lack of phenotype is also consistent with previous data that have shown that a reduction in the levels of the SMC proteins does not affect the properties of the chromosome arm [68].

tDNAs and chromosome structure

The 275 tDNAs in the yeast genome are dispersed across the sixteen chromosomes, but two thirds of these tDNAs cluster together at two sites in the genome. It has been speculated that this spatial organization is a driver of chromosome folding and packaging [118, 119], though the extent to which this occurs has remained unclear. Our Micro-C analysis of chromosome III suggests that tDNAs are unlikely to be drivers of chromosome folding and condensation. Genome compaction driven by the underlying DNA sequence as well as tethering of centromeres and telomeres likely results in the clustering of tDNAs in 3D space. It is therefore more likely that the tDNA clustering observed by microscopy as well as by proximity based ligation is a function of the linear proximity of tDNAs along the chromosome. tDNAs are often syntenic along chromosomes with respect to flanking RNA pol II transcribed genes [44, 149], and it is possible that these positions have been selected for optimal gene activity rather than being a driver of chromosome folding [150].

The yeast chromosomes have isochores with G-C rich, gene rich R-band segments alternating with AT-rich G-band segments [151, 152], which exhibit different functional properties [153, 154]. Chromosome III has a G-C segment from 20 to 100

kb on the left arm, followed by an A-T rich central segment from 100 to 200kb on the right arm, and then a second G-C rich segment from 200 to 290kb on the same arm. Mapping of the double strand breaks and recombination hot spots that occur in meiosis [155, 156] show a dramatic reduction in break formation and recombination in the A-T rich isochore. The 3D structure of chromosome III shows that the central A-T rich segment is stiff and exhibits less curvature compared to the flanking gene rich G-C rich segments [63]. The A-T rich segment is precisely the region rich in tDNAs (See Figure1), and tDNAs are constitutively active genes that strongly associate with nuclear pores [157]. The tethering of sequence elements to nuclear substructures is important in nuclear organization. The underlying A-T rich DNA sequence likely plays a dominant role in the 3D folding of this segment, but it is possible that tDNAs play a role in the tethering of this segment. The effects of the tDNA deletion on mobility occur at the boundary of the A-T rich isochore with a change in the mobility at the *MAT* locus and *BUD31*, though the left boundary of this isochore does not show a change in mobility most likely because this is close to the centromere. Thus, tDNAs in this segment via their association to nuclear structures could affect how this segment relates to the flanking G-C rich segments. Loss of the tDNAs could thus affect the flexibility between the segments without affecting the overall macro-folding of the chromosome.

tDNAs and centromere clustering

Nuclear organization is primarily driven by chromosome tethering to nuclear substructures [87]. The key DNA sequences that tether chromosomes and organize

the yeast nucleus are the centromeres and the telomeres [48]. Proteins bound to these DNA sequences make contact with nuclear membrane proteins to anchor chromosomes and thereby help organize the nucleus [51, 52, 91-93, 130, 158-161].

All sixteen centromeres cluster together in a ring around the membrane embedded spindle pole body. The centromeres are tethered to the spindle pole body via direct interactions between kinetochore-associated proteins and the spindle pole body associated microtubules [51, 63, 130, 158]. It has been assumed that tethering the 16 centromeres to the spindle pole body results in centromere clustering, but not much is known about other factors that influence this phenomenon.

Our observation that loss of tDNAs results in increased interactions between the clustered centromeres provides a clear demonstration of a novel cis acting element that affects centromere clustering. tDNAs are not present in the immediate vicinity of the chromosome III centromere, but tDNA density is almost 2 fold higher in the pericentric region of *S. cerevisiae* chromosomes including chromosome III [78] (see Figure 1). HiC data show that approximately a third of all of the tDNAs localize near the centromeres in 3D space [52]. Furthermore, tDNAs have been shown to help tether centromeres to the spindle axis during mitosis [78].

Our data indicate that the physical presence of tDNAs in the pericentric region of the chromosome prevents close packaging of centromeres during interphase. This could be due to transcription-mediated effects since tRNA genes are highly active and these genes cluster together around the centromeres. Thus, tDNA-tDNA clustering at RNA pol III transcription factories near the centromeres could hinder closer

centromere-centromere interactions. An alternative possibility is based on the observation that transcriptionally active tDNAs interact with nuclear pores [55, 84, 157]. It is thus possible that there is a competition between tDNA- nuclear pore interactions and centromere-centromere interactions. In this scenario, the loss of tDNA tethering to the nuclear pore would enable the centromere greater freedom of movement thus enabling closer centromere-centromere interactions. Irrespective of the exact model of how tDNAs affect centromere clustering it should be noted that there are parallels between distinct factors being required for tethering and clustering. Telomeres are anchored to the nuclear membrane via interactions between telomere and subtelomere bound proteins to proteins in the inner nuclear membrane. Clustering of telomeres on the other hand is dependent upon silencing of sub-telomeric sequences and the length of the chromosome arms [57, 59, 162]. While clustering of telomeres is lost when tethering is reduced, tethering is not abolished when clustering is reduced.

tDNA effects on *HML-HMR* interactions and the inheritance of gene silencing

Gene silencing is primarily a function of the Sir proteins, though numerous other factors influence the process [163]. Once silencing is established, the silent state is faithfully and efficiently propagated following DNA replication, and many of the factors involved in this process have been identified [60, 133, 164-169].

Proto-silencers are sequence elements that on their own are unable to silence a gene, but when located near a silencer increase the efficiency of silencing [170, 171].

Our demonstration that the tDNA affects silencing of a reporter adjacent to the silent *HMR* domain was not very surprising since a tDNA resides very close to this site and is anchored to the nuclear pore [55]. What was unexpected was the observation that loss of this tDNA led to a reduction in silencing at both the *HMR* and the *HML* locus. A reduction in silencing at *HMR* could be ascribed to a local effect of the tDNA recruiting the adjacent *HMR* locus to the nuclear periphery since this is a compartment rich in silencing proteins. The *HML* locus however resides over 300 kb from *HMR* and there are no tDNAs in its vicinity. The closest tDNA is approximately 71 kb from *HML*. We showed that the loss of the tDNA at *HMR* results in a reduction of long-range *HML-HMR* interactions, and a reduction in silencing of the reporter just outside of *HML*. The most parsimonious explanation of this observation is that the loss of *HML-HMR* interaction in turn leads to reduction in gene silencing at *HML*. If this were indeed the case, then the data would argue that tDNA mediated clustering of silent loci is important in the silencing of these loci and the loss of long-range association might reduce the efficient inheritance of the silent state. This is analogous to the observations that gene clustering at active chromatin hubs and transcription factories increases the efficiency of transcription. The data are also consistent with the observations that telomere clustering increases the efficiency of silencing at sub-telomeric sequences [172].

This unexpected observation also raises the question of how tDNAs may influence long-range *HML-HMR* interactions. tDNAs, including the tDNA next to *HMR,* are sites of replication slowing/pausing [173-178]. The tDNA adjacent to *HMR*

is enriched in SMC proteins [1, 145], and tDNAs generally are enriched in γ-H2A [2, 148]. We recently showed that long-range *HML-HMR* interactions require homologous sequences to be present at these loci. Mutations in replication coupled homologous recombination repair proteins, including the SMC proteins and γ-H2A, lead to a reduction in *HML-HMR* interactions [1, 18]. Based on the accumulated data, we would posit that replication fork slowing/pausing results in the deposition of γ-H2A and SMC proteins followed by a homology search leading to *HML-HMR* interactions. The re-formation of silenced chromatin following replication precludes the eviction of γ-H2A [179] thereby stabilizing SMC protein binding, which then maintains the long-range *HML-HMR* association. The tDNAs thus help establish a network of interactions mediated by the SMC proteins and the Sir proteins leading to *HML-HMR* association and chromosome folding. The data also suggest that a series of transient interactions, most likely during replication, aid in the setting up of the final optimal nuclear architecture found in the interphase nucleus.

It should be borne in mind that, in this study, we solely investigated tDNAs and their role in nuclear architecture in *S. cerevisiae*, but other repetitive DNA sequences (along with tDNAs) could play analogous roles in metazoans. Alu and SINE elements are some of the most abundant sequence elements in mammals. These sequences, as well as tDNAs, all bind pol III transcription factors and function as gene insulators [44, 110, 180, 181]. Some of these sequences are also found at the boundaries of TADs [17, 34]. Furthermore, tDNAs cluster together over long distances forming chromatin loops [44, 117], and these and other repetitive sequences are sites of

replication fork pausing in mammalian cells [14, 182-186]. Given these commonalities it is possible and even likely that similar mechanisms to the ones described in *S. cerevisiae* play a role in setting up the nuclear architecture in larger eukaryotes. Loss of these sequence elements could also have unpredictable effects affecting diverse nuclear processes. The goal of building synthetic genomes lacking repetitive DNA sequences may lead to unexpected alterations in nuclear architecture and gene regulation [187].

Materials and Methods

Yeast strains and primers

Table S1 and S2 list the yeast strains and the primer sequences that were used in this study.

MNase-Seq

MNase-Seq experiments were carried out as previously described [100]. In brief, chromatin that was isolated from a strain of interest was subjected to MNase digestion in order to achieve a desired size of DNA in the range of about one nucleosome, or ~150 bp's. The DNA was then isolated from the chromatin samples, and paired-end high-throughput sequencing libraries were prepared (Illumina). These libraries were then sequenced using an Illumina high-throughput sequencing platform, and the paired-end reads were mapped back to a budding yeast reference genome (SacCer_Apr2011/sacCer3) [188-190]. The mapping results gave nucleosome-level resolution on the placement of nucleosomes throughout the genome

of a given strain. For the analysis of nucleosome occupancy at tDNAs, both across the genome and on chromosome III, tDNAs were aligned at their transcriptional start sites, and the nucleosome position cluster density was averaged for each tDNA in order to generate the data on nucleosome position clusters at tDNAs.

ChIP

ChIP-qPCR experiments on Brn1 and Scc2/4 were performed as previously described [1, 83]. In brief, yeast cells of a strain of interest were inoculated and grown overnight in 300 ml of YPD media to an OD of 1-2. These cells were then fixed in 1% formaldehyde for a duration of 2 hours at room temperature. The reaction was then quenched with glycine, and the cells were spun down and washed in 1X PBS. The cross linked cells were then flash frozen in dry ice and stored at -70^{0}C. In preparation for IP, the cells were thawed on ice, broken apart by bead beating, and sonicated to achieve a desired chromatin size of ~300 bp. Once the size of the chromatin was checked, cell debris were cleared from the sample by high-speed centrifugation. The crosslinked, sized chromatin was split into 2 samples and IPs were done overnight in the presence of both an antibody to the protein of interest as well as pre-blocked A/G-Sepharose beads at 4^{o}C. 50 µl of input chromatin was also taken from each IP sample prior to addition of the antibody. Chromatin elution was done using 10% Chelex 100 (Bio-Rad) along with proteinase K treatment. After elution, both input and IP DNA were quantitated via a Picogreen fluorescent quantification assay (Invitrogen). For each qPCR reaction, input DNA was run in triplicate and IP DNA was run in duplicate. An equal amount of input and IP DNA

was used in each individual reaction. The enrichment for a given probe was then calculated as IP/Input, and was further normalized to the OCA4 locus. The results of each ChIP-qPCR are comprised from two independent crosslinks per strain assayed, and for each crosslink two independent IPs were done.

Mean Squared Distance Analysis

Mean-squared distance analysis was carried out as previously described [21, 128, 191]. In brief, we built strains that contained a 64x lacO array at specific points along chromosome III. We then integrated a cassette containing an spc29-RFP fusion protein elsewhere in the genome. This protein is an essential kinetochore protein, and therefore serves as a marker for the spindle pole body. The spindle pole body served as a fixed point to which we could measure the movement of our GFP tagged loci in 3D space over a period of 10 minutes. Positional data on the location of the GFP dot is recorded at 30-second increments, and that data is used to calculate the radius of constraint (Rc) for a specific locus in a given strain (WT or tDNA delete). This analysis was performed in no less than 35 cells per genotype assayed. Data for each genotype were also composed of two independent strains per genotype.

HML-HMR Colocalization analysis

Distance assays between *HML* and *HMR* were performed as previously described [1].

Single Cell Expression Analysis

Single cell expression analysis was performed as previously described [133].

Micro-C

Micro-C was performed as previously described [35, 129]. In brief, this technique provides nucleosome level resolution of all of the interactions occurring across the genome by using MNase digestion in lieu of a restriction enzyme as in traditional Hi-C techniques.

Antibodies

Antibodies used in ChIP were as follows; Scc2-Myc: anti-myc 9E10 (Abcam) = 5 µl, Brn1-HA: anti-HA HA.11 (Covance) = 5 µl.

Figures

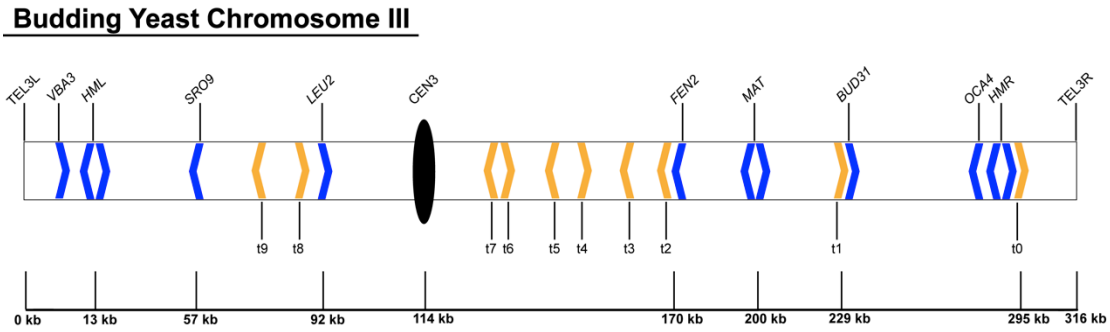

Figure 1. **Schematic of Budding Yeast Chromosome III**. The relative positions of loci on chr III are represented by the scale below the chromosome. The locations of all 10 tDNAs on chromosome III are displayed. tDNAs are denoted by the yellow arrowheads. The direction of the arrowhead denotes the direction of transcription. Other loci of interest in this study are marked by the blue arrowheads.

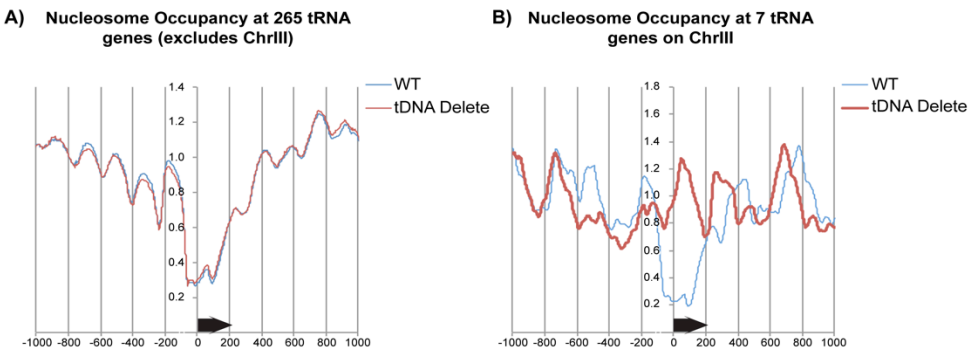

Figure 2. **Deletion of tDNAs across budding yeast chromosome III leads to local changes in nucleosome structure surrounding tDNAs.** The data displayed are from a series of MNase-seq experiments. A.) Data displayed are for a comparison of nucleosome occupancy at 265 tDNAs that have been aligned by their transcriptional start site, excluding chromosome III tDNAs. The nucleosome phasing pattern is displayed for both WT (blue) and tDNA delete (red). The black arrow denotes the direction of transcription that was used to align the tDNAs. B.) Data displayed are for comparison of the nucleosome occupancy at tDNAs across chromosome III. These data are representative of 2 independent biological replicates.

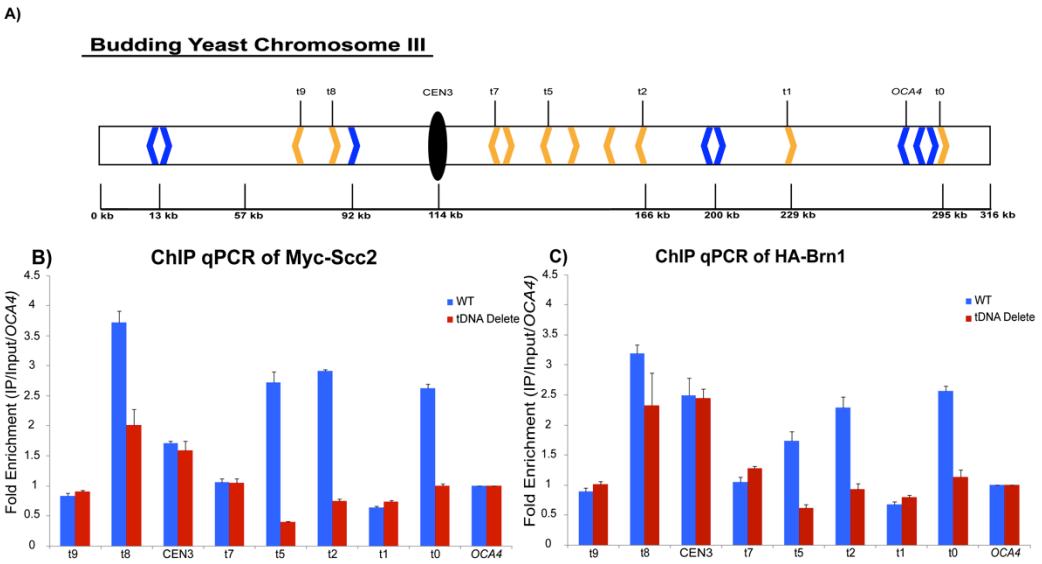

Figure 3. **tDNAs differentially recruit both Scc2 and Condensin. (**A) Figure shows a schematic of budding yeast chromosome III with loci of interest for the ChIP experiments that were carried out. The locations of ChIP-qPCR amplicons that were used are denoted along the chromosome. (B) Graph showing enrichment values for ChIP-qPCR mapping of Myc-Scc2. These data are the results of 2 biological replicates. Two IPs were done for each biological replicate. A percentage of input value was first calculated for each amplicon, which was then normalized to the OCA4 locus. Error bars represent standard error. (C) Graph showing ChIP-qPCR mapping of HA-Brn1, condensin. Data were calculated in the same way as for the Scc2 ChIP, and normalized to the OCA4 locus.

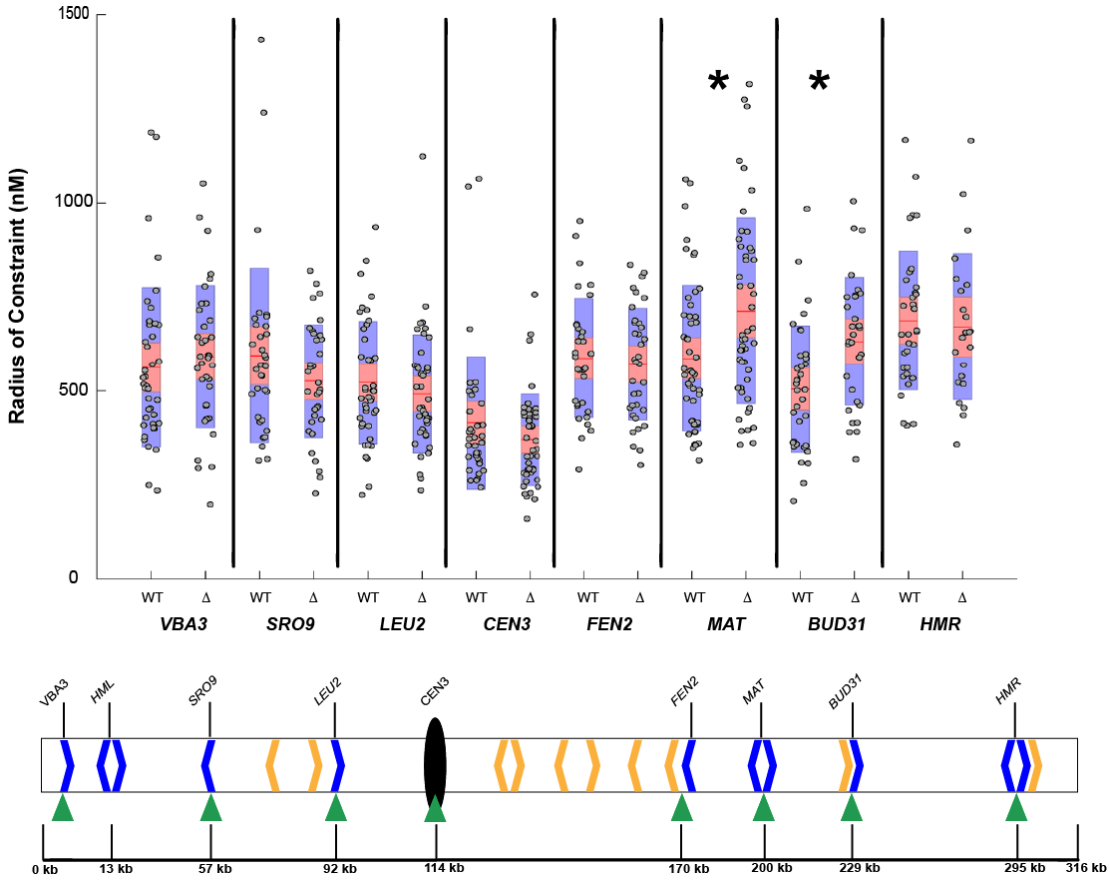

Figure 4. Deletion of **tDNAs from budding yeast chromosome III leads to increased mobility.** Box plots represent the data obtained from MSD experiments. Components of each boxplot are as follows; red line is the mean, pink bar is the 95% confidence interval, purple bar is the standard deviation, and the grey dots represent individual values obtained from a single experiment. The locations of the 8 loci that were assayed are denoted by the green arrowheads beneath the chromosome III schematic. The radius of constraint (Rc) measurement was calculated from MSD graphs that were generated over the course of a 10 minute time-lapse movie. These experiments are the result of time-lapse images taken from at least 35 cells per locus assayed. A "*" above the bars of a locus on the graph denotes a statistically significant difference between WT and tDNA delete according to a 2-sample, 2-tailed t-test assuming unequal variance ($p<0.05$).

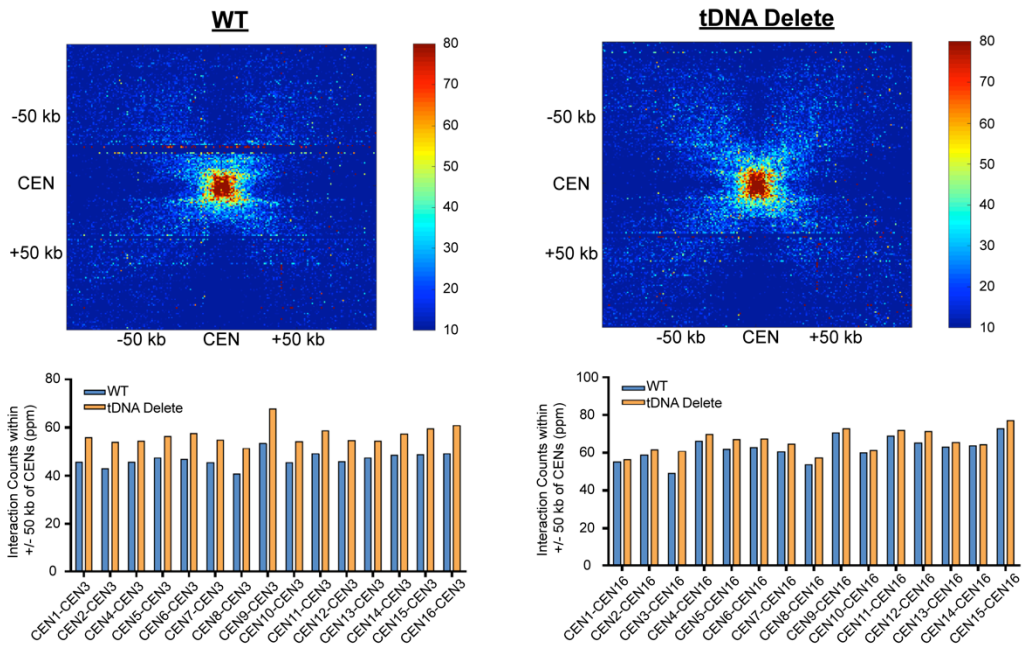

Figure 5A. **Deletion of tDNAs from chromosome III leads to an increase in CEN3 interaction with all other centromeres in the genome.** Data shown are an analysis of CEN-CEN interactions. The heatmaps display a piled alignment of all centromeres throughout the genome. Interaction frequencies are denoted by the colored bar to the right of each heatmap. The graphs below the heatmaps are quantification of CEN-CEN interactions. The right graph examines the interaction of CEN16 with all other CENs, and the left graph examines the interaction of CEN3 with all other CENs. The y-axis is given in interaction counts within 50 kb of each CEN in parts per million (ppm), which shows interaction between a pair of genomic loci per million reads.

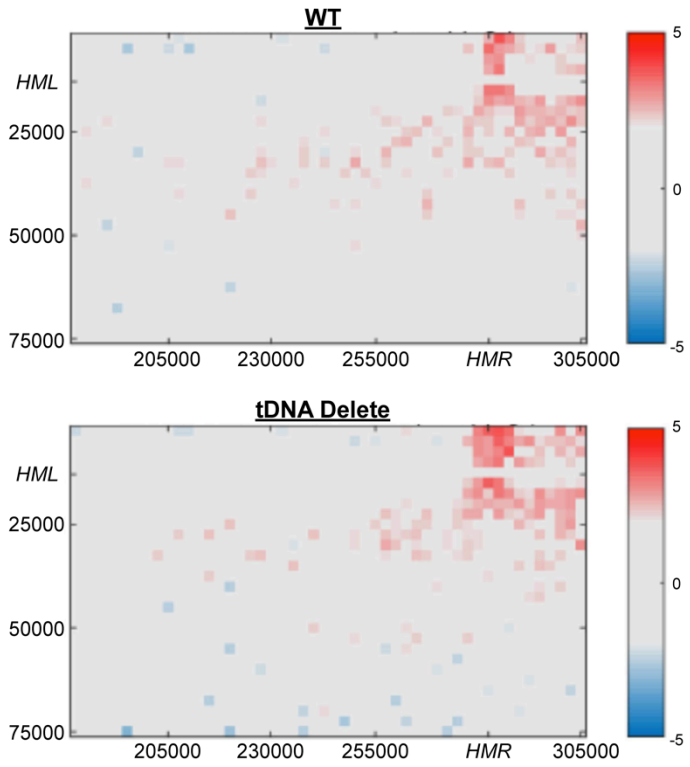

Figure 5B. **Deletion of tDNAs on chromosome III leads to a change in *HML-HMR* interaction.** These heatmaps display the interaction profile between the areas on chromosome III surrounding *HML* and *HMR* that were obtained from Micro-C data. Increased interactions are denoted by red and decreased interactions are denoted by blue. The data are displayed in a log2 format. The x and y axes denote the area of the chromosome displayed on each axis of the heat map.

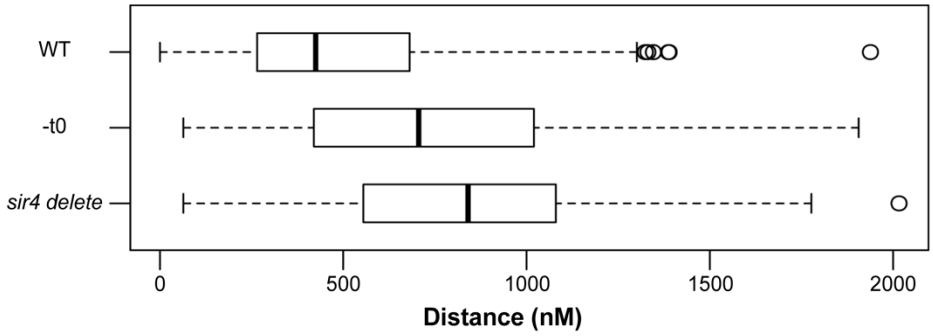

Figure 5C. **Deletion of tDNA t0 leads to perturbation of *HML-HMR* long-range association.** These boxplots show data on the distances between TetR-YFP and CFP-LacI foci in asynchronously growing yeast cells. Data were acquired from at least 150 cells for each genotype. The dark line in the middle of the box represents the median distance. The lower end of the box represents the 25th percentile of the data, and extends up to the upper end of the box that represents the 75th percentile of the data. The upper and lower ends of the whiskers denote the 2.5th and 97.5th percentile of the data respectively.

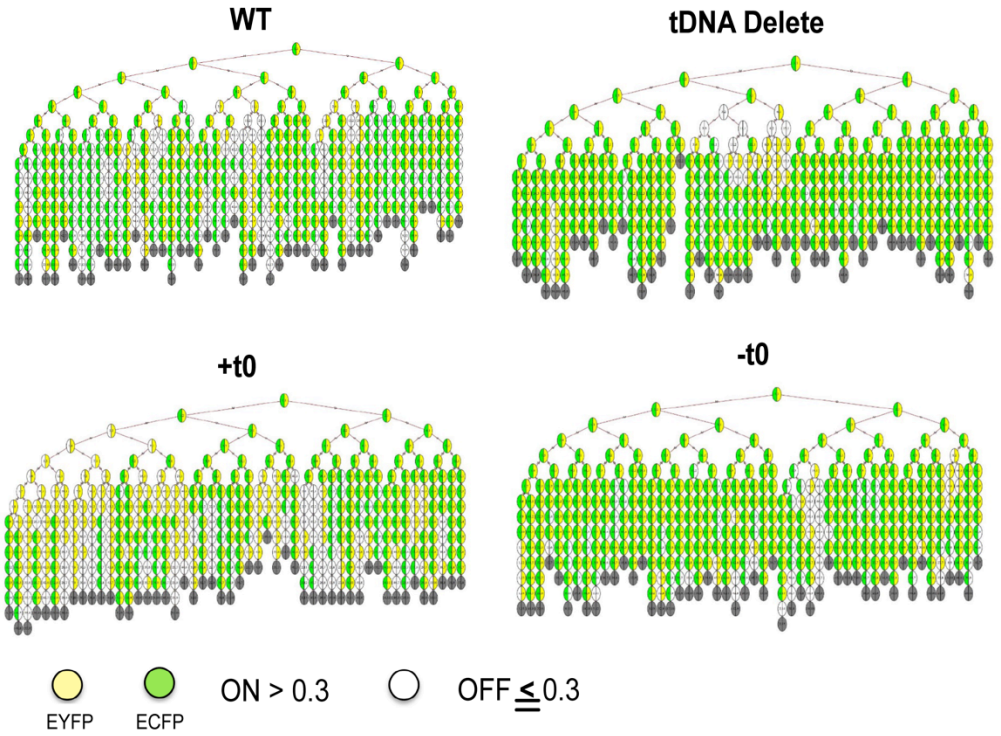

Figure 6A. t**DNAs on chromosome III modulate silencing of reporter genes at *HML* and *HMR*.** Representative lineage trees are shown for the 4 different genotypes that were used for this assay. The expression of HML::EYFP or HMR::ECFP in each generation of cells is indicated by the presence of their respective colors in the cells of the tree.

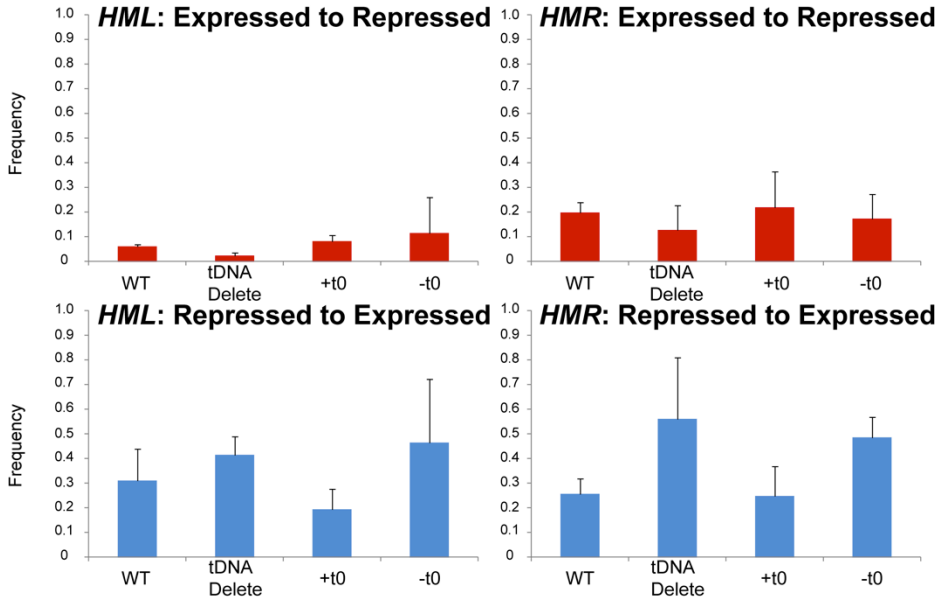

Figure 6B. **Deletion of tDNAs on chromosome III leads to a change in silencing maintenance at reporter genes placed at *HML* and *HMR*.** The graphs quantify the changes in expression state of HML::EYFP and HMR::ECFP between cell generations. Expressed to repressed transitions represent a reporter that was expressed in one generation and not expressed in the next. Repressed to expressed transitions represent a reporter gene that was not expressed in one generation and expressed in the next. The data reported are in frequency.

Table S1. Yeast strains used in this study.

Strain	Genotype Information	Experiment
JKY562	MATa t0D, t1D, t2D, t3D, t4D, t5D, t6D, t7D, t8D+t9D T1+T7::HIS3 Laci-GFP::ADE2 LEU2 BRN1-HA::KanMx	ChIP-qPCR
JKY702	MATa t0D, t1D, t2D, t3D, t4D, t5D, t6D, t7D, t8D+t9D T1+T7::HIS3 Mcd1-13xMyc::KanMx LacI-GFP::ADE2	ChIP-qPCR
ROY4825	MATa HMR(s288c) SCC2-13XMyc::KanMx ADE2 his3 leu2 lys2 trp1 ura3	ChIP-qPCR
ROY4925	MATa HMR(s288c) Mcd1-13Xmyc::KanMx ADE2	ChIP-qPCR
ROY4927	MATα HMR(s288c) BRN1-HA::KanMx ADE	ChIP-qPCR
ROY5151	t0D, t1D, t2D, t3D, t4D, t5D, t6D, t7D, t8D+t9D::LEU2 T1+T7::HIS3 MATa ade2- LYS2+ SCC2-13xMyc::KanMx	ChIP-qPCR
ROY5288	MATa LacI-GFP::ADE2 126xLacO::CEN3::TRP1 spc29-RFP::Hyg	MSD
ROY5289	MATa LacI-GFP::ADE2 126xLacO::CEN3::TRP1 spc29-RFP::Hyg	MSD
ROY5290	MAT@ LacI-GFP::ADE2 126xLacO::CEN3::TRP1 spc29-RFP::Hyg t0D, t1D, t2D, t3D, t4D, t5D, t6D, t7D, t8D+t9D T1+T7::HIS3 leu2-	MSD
ROY5291	MAT@ LacI-GFP::ADE2 64xLacO::CEN3::TRP1 spc29-RFP::Hyg t0D, t1D, t2D, t3D, t4D, t5D, t6D, t7D, t8D+t9D T1+T7::HIS3 leu2-	MSD

ROY5294	MAT@ LacI-GFP::ADE2 MAT::LacO::TRP1 lys- SPC29-RFP::Hyg	MSD
ROY5317	MAT@ LacI-GFP::ADE2 lys-56xLacO::LEU2 SPC29-RFP::Hyg	MSD
ROY5318	MAT@ LacI-GFP::ADE2 lys-56xLacO::LEU2 SPC29-RFP::Hyg	MSD
ROY5319	MAT@ LacI-GFP::ADE2 lys-MAT::LacO::TRP1 SPC29-RFP::Hyg t0D, t1D, t2D, t3D, t4D, t5D, t6D, t7D, t8D+t9D::LEU2 T1+T7::HIS3	MSD
ROY5320	MAT@ LacI-GFP::ADE2 lys-MAT::LacO::TRP1 SPC29-RFP::Hyg t0D, t1D, t2D, t3D, t4D, t5D, t6D, t7D, t8D+t9D::LEU2 T1+T7::HIS3	MSD
ROY5321	MAT@ LacI-GFP::ADE2 lys-GIT1::56xLacO::TRP1 SPC29-RFP::Hyg t0D, t1D, t2D, t3D, t4D, t5D, t6D, t7D, t8D+t9D::LEU2 T1+T7::HIS3	MSD
ROY5323	MAT@ LacI-GFP::ADE2 lys-GIT1::56xLacO::TRP1 SPC29-RFP::Hyg t0D, t1D, t2D, t3D, t4D, t5D, t6D, t7D, t8D+t9D::LEU2 T1+T7::HIS3	MSD
ROY5359	MAT@ LacI-GFP::ADE2 lys-MAT::LacO::TRP1 SPC29-RFP::Hyg	MSD
ROY5664	LacI-GFP::ADE2 GIT1::56xLacO::TRP1 SPC29-RFP::Hyg	MSD
ROY5665	LacI-GFP::ADE2 GIT1::56xLacO::TRP1 SPC29-RFP::Hyg	MSD
ROY5666	LacI-GFP::ADE2 t1wt::56xLacO::LEU2 SPC29-RFP::Hyg	MSD
ROY5667	LacI-GFP::ADE2 t1wt::56xLacO::LEU2 SPC29-RFP::Hyg	MSD

ROY5668	LacI-GFP::ADE2 t2wt::56xLacO::LEU2 SPC29-RFP::Hyg	MSD
ROY5669	LacI-GFP::ADE2 t2wt::56xLacO::LEU2 SPC29-RFP::Hyg	MSD
ROY5670	LacI-GFP::ADE2 TEL3L::LacO::TRP1 SPC29-RFP::Hyg	MSD
ROY5671	LacI-GFP::ADE2 TEL3L::LacO::TRP1 SPC29-RFP::Hyg	MSD
ROY5672	LacI-GFP::ADE2 Chr3L(mid)::LacO::TRP1 SPC29-RFP::Hyg	MSD
ROY5687	LacI-GFP::ADE2 t1::56xLacO::LEU2 SPC29-RFP::Hyg t0D, t1D, t2D, t3D, t4D, t5D, t6D, t7D, t8D+t9D T1+T7::HIS3 leu2-	MSD
ROY5688	LacI-GFP::ADE2 t1::56xLacO::LEU2 SPC29-RFP::Hyg t0D, t1D, t2D, t3D, t4D, t5D, t6D, t7D, t8D+t9D T1+T7::HIS3 leu2-	MSD
ROY5689	LacI-GFP::ADE2 56xLacO::LEU2 SPC29-RFP::Hyg t0D, t1D, t2D, t3D, t4D, t5D, t6D, t7D, t8D+t9D T1+T7::HIS3	MSD
ROY5690	LacI-GFP::ADE2 56xLacO::LEU2 SPC29-RFP::Hyg t0D, t1D, t2D, t3D, t4D, t5D, t6D, t7D, t8D+t9D T1+T7::HIS3	MSD
ROY5695	LacI-GFP::ADE2 lys2-Chr3L(mid)::LacO::TRP1 SPC29-RFP::Hyg t0D, t1D, t2D, t3D, t4D, t5D, t6D, t7D, t8D+t9D::LEU2 T1+T7::HIS3	MSD
ROY5696	LacI-GFP::ADE2 lys2-Chr3L(mid)::LacO::TRP1 SPC29-RFP::Hyg t0D, t1D, t2D, t3D, t4D, t5D, t6D, t7D, t8D+t9D::LEU2 T1+T7::HIS3	MSD

ROY5748	MATa LacI-GFP::ADE2 t2::56xLacO::LEU2 SPC29-RFP::Hyg t0D, t1D, t2D, t3D, t4D, t5D, t6D, t7D, t8D+t9D T1+T7::HIS3 leu2-	MSD
ROY5749	MATa LacI-GFP::ADE2 t2::56xLacO::LEU2 SPC29-RFP::Hyg t0D, t1D, t2D, t3D, t4D, t5D, t6D, t7D, t8D+t9D T1+T7::HIS3 leu2-	MSD
ROY5750	MATa LacI-GFP::ADE2 lys2-TEL3L::LacO::TRP1 SPC29-RFP::Hyg t0D, t1D, t2D, t3D, t4D, t5D, t6D, t7D, t8D+t9D::LEU2? T1+T7::HIS3	MSD
ROY5751	MATa LacI-GFP::ADE2 lys2-TEL3L::LacO::TRP1 SPC29-RFP::Hyg t0D, t1D, t2D, t3D, t4D, t5D, t6D, t7D, t8D+t9D::LEU2? T1+T7::HIS3	MSD
GRY823	Mata LacI-GFP::ADE2 LacO(64x)::CEN3::TRP1	Meiotic Crossover Analysis
GRY824	MAT@ LacI-GFP::ADE2 LacO(64x)::CEN3::TRP1	Meiotic Crossover Analysis
GRY872	MAT@ 126xLacO::CEN3::TRP1 t0D, t1D, t2D, t3D, t4D, t5D, t6D, t7D, t8D+t9D T1+T7::HIS3 leu2-3, 112 LacI-GFP::ADE2 trp- lys- ura-	Meiotic Crossover Analysis
GRY883	MAT@ t1WT@HIS3 chr3t1WT::URA3 GIT1::TRP1 LYS+ LEU+ ade-	Meiotic Crossover Analysis
GRY907	MAT@ LacI-GFP::ADE2 56xLacO::LEU2 lys- trp- ura- his-	Meiotic Crossover Analysis
GRY911	MATa LacI-GFP::ADE2 56xLacO::LEU2 lys-	Meiotic Crossover Analysis

GRY935	MATa LacI-GFP::ADE2 t0D, t1D, t2D, t3D, t4D, t5D, t6D, t7D, t8D+t9D T1+T7::HIS3 trp- leu- lys- ura-	Meiotic Crossover Analysis
GRY938	MAT@ B1Δ::URA3 t0D, t1D, t2D, t3D, t4D, t5D, t6D, t7D, t8D+t9D::LEU2 T1+T7::HIS3 LacI-GFP::ADE2 HMR-GIT1::TRP1 lys-	Meiotic Crossover Analysis
GRY963	MAT@ t0D, t1D, t2D, t3D, t4D, t5D, t6D, t7D, t8D+t9D T1+T7::HIS3 LYS+ ade- leu-	Meiotic Crossover Analysis
JRY4012	MATa can1-100 his3-11 leu2-3,112 lys2Δ trp1-1 ura3-1 GAL	Meiotic Crossover Analysis
ROY5510	MAT@ lys- LacI-GFP::ADE2 t2wt::56xLacO::LEU2	Meiotic Crossover Analysis
ROY5512	MATa LacI-GFP::ADE2 t2::56xLacO::LEU2 t0D, t1D, t2D, t3D, t4D, t5D, t6D, t7D, t8D+t9D T1+T7::HIS3 leu2-	Meiotic Crossover Analysis
ROY5518	MATa LacI-GFP::ADE2 lys2-Chr3L(mid)::LacO::TRP1 t0D, t1D, t2D, t3D, t4D, t5D, t6D, t7D, t8D+t9D::LEU2 T1+T7::HIS3	Meiotic Crossover Analysis
ROY5521	MATa lys- LacI-GFP::ADE2 Chr3L(mid)::LacO::TRP1	Meiotic Crossover Analysis
ROY5602	MATa LacI-GFP::ADE2 56xLacO::LEU2 t0D, t1D, t2D, t3D, t4D, t5D, t6D, t7D, t8D+t9D T1+T7::HIS3	Meiotic Crossover Analysis
JKY689	MATa tDNA0 (WT) t1D, t2D, t3D, t4D, t5D, t6D, t7D, t8D+t9D T1+T7::HIS3 LEU2 ade2-1	Single Cell Expression Analysis
ROY1681	MAT@ ADE2 his3 leu2 lys2 trp1 ura3 HMR (t-RNA bound delete)	Single Cell Expression Analysis
WT = JRY2334?	MATa ade2-1 can1-100 his3-11 leu2-3,112 trp1-1 ura3-1 GAL	Single Cell Expression Analysis

JKY690	MATa t0D, t1D, t2D, t3D, t4D, t5D, t6D, t7D, t8D+t9D T1+T7::HIS3 LEU2 ade2-1 LYS+	Micro-C / MNase Seq
JRY2334	MATa ade2-1 can1-100 his3-11 leu2-3,112 trp1-1 ura3-1 GAL	Micro-C / MNase Seq
ROY4830	MATa/MAT@ HML-TetO :: LEU2 HMR-LacO:: TRP1 CFP-LacI-TetR-YFP::ADE2 LYS2	Colocalization Assay
ROY4846	MAT@ LacO(256x)::GIT1::TRP1 HML-TetO::LEU2 CFP-LacI-TetR-YFP::ADE2 tT(AGU)CΔ::URA3 lys2Δ	Colocalization Assay
ROY4859	MAT HML-tetO::LEU2 HMR-LacO::TRP1 CFP-LacI-TetR-YFP::ADE2 sir4Δ::URA3 lys-	Colocalization Assay
ROY4860	MAT HML-tetO::LEU2 HMR-LacO::TRP1 CFP-LacI-TetR-YFP::ADE2 sir4Δ::URA3 lys-	

Table S2. qPCR primers used in this study.

Primer Name	**Sequence 5'-3'**	**Amplicon**
yOH58	TACTACAAGAGAAAGGCCATCTCC	t1
yOH59	AATGCAGCGCAGACAGCACAGTT	t1
QJK61	TTGAGATACAAAATATTACAAGAAGTCCTG	t2
QJK62	GCGTTCTTCTGTATCTGAAGATAGTG	t2
QJK63	TCATGTATCAAGATTACTAGCGCAAGTG	t5
QJK64	TTCTATTCTTATGTACCGTTCCGCC	t5
yOH62	GCAAGCGAAGTTGTTCCCGTTAT	t7
yOH63	GTTCGGTCACTTAGAGGATATAATTG	t7
QJK69	CTCTATTTCTCAACAAGTAATTGGTTGTTT	t8
QJK70	GCCCCTGTGTGTTCTCGTTATGT	t8
yOH64	GACAAGAAAGATAACGACACAGTGA	t9
yOH65	GGCCCTCGTATAGTCTCTTTTC	t9
R197	GAGACCAGGTTTATTCAACCGGTAAC	t0
LOU120	GGGTGTCACCGAATAACGTGAT	t0
GRO39	TAAGACAATTGTGGACAACAAAGCAAA	*OCA4*
GRO40	ATTTATTAATGTCAAAAGCCGCTGAGG	*OCA4*
yOH66	TCACTCATATAAACCGAACCCTTCC	CEN3
yOH67	GGATTTTCCATATTGTTTGGCGCTG	CEN3

References

1. Kirkland, J.G. and R.T. Kamakaka, *Long-range heterochromatin association is mediated by silencing and double-strand DNA break repair proteins.* J Cell Biol, 2013. **201**(6): p. 809-26.
2. Szilard, R.K., et al., *Systematic identification of fragile sites via genome-wide location analysis of gamma-H2AX.* Nat Struct Mol Biol, 2010. **17**(3): p. 299-305.
3. Pinto, D.M. and A. Flaus, *Structure and function of histone H2AX.* Subcell Biochem, 2010. **50**: p. 55-78.
4. Lieberman-Aiden, E., et al., *Comprehensive mapping of long-range interactions reveals folding principles of the human genome.* Science, 2009. **326**(5950): p. 289-93.
5. Goodarzi, A.A., P. Jeggo, and M. Lobrich, *The influence of heterochromatin on DNA double strand break repair: Getting the strong, silent type to relax.* DNA Repair (Amst), 2010. **9**(12): p. 1273-82.
6. Stucki, M., et al., *MDC1 directly binds phosphorylated histone H2AX to regulate cellular responses to DNA double-strand breaks.* Cell, 2005. **123**(7): p. 1213-26.
7. Altmeyer, M. and J. Lukas, *To spread or not to spread--chromatin modifications in response to DNA damage.* Curr Opin Genet Dev, 2013. **23**(2): p. 156-65.
8. Lukas, J., C. Lukas, and J. Bartek, *More than just a focus: The chromatin response to DNA damage and its role in genome integrity maintenance.* Nat Cell Biol, 2011. **13**(10): p. 1161-9.
9. West, M.H. and W.M. Bonner, *Histone 2A, a heteromorphous family of eight protein species.* Biochemistry, 1980. **19**(14): p. 3238-45.
10. Rogakou, E.P., et al., *DNA double-stranded breaks induce histone H2AX phosphorylation on serine 139.* J Biol Chem, 1998. **273**(10): p. 5858-68.
11. Boyarchuk, E., R. Montes de Oca, and G. Almouzni, *Cell cycle dynamics of histone variants at the centromere, a model for chromosomal landmarks.* Curr Opin Cell Biol, 2011. **23**(3): p. 266-76.
12. Redon, C., et al., *Histone H2A variants H2AX and H2AZ.* Curr Opin Genet Dev, 2002. **12**(2): p. 162-9.
13. Rogakou, E.P., et al., *Megabase chromatin domains involved in DNA double-strand breaks in vivo.* J Cell Biol, 1999. **146**(5): p. 905-16.
14. Barlow, J.H., et al., *Identification of early replicating fragile sites that contribute to genome instability.* Cell, 2013. **152**(3): p. 620-32.
15. Caron, P., et al., *Cohesin protects genes against gammaH2AX Induced by DNA double-strand breaks.* PLoS Genet, 2012. **8**(1): p. e1002460.
16. Bewersdorf, J., B.T. Bennett, and K.L. Knight, *H2AX chromatin structures and their response to DNA damage revealed by 4Pi microscopy.* Proc Natl Acad Sci U S A, 2006. **103**(48): p. 18137-42.

17. Dixon, J.R., et al., *Topological domains in mammalian genomes identified by analysis of chromatin interactions.* Nature, 2012. **485**(7398): p. 376-80.
18. Kirkland, J., et al., *Heterochromatin formation via recruitment of DNA repair proteins.* Molecular Biology of Cell, 2015.
19. Rozenzhak, S., et al., *Rad3 decorates critical chromosomal domains with gammaH2A to protect genome integrity during S-Phase in fission yeast.* PLoS Genet, 2010. **6**(7): p. e1001032.
20. Swaminathan, J., E.M. Baxter, and V.G. Corces, *The role of histone H2Av variant replacement and histone H4 acetylation in the establishment of Drosophila heterochromatin.* Genes Dev, 2005. **19**(1): p. 65-76.
21. Hediger, F., et al., *Live Imaging of Telomeres. yKu and Sir Proteins Define Redundant Telomere-Anchoring Pathways in Yeast.* Curr Biol, 2002. **12**(24): p. 2076-89.
22. Ribes-Zamora, A., et al., *TRF2 interaction with Ku heterotetramerization interface gives insight into c-NHEJ prevention at human telomeres.* Cell Rep, 2013. **5**(1): p. 194-206.
23. Ohta, T., K. Sato, and W. Wu, *The BRCA1 ubiquitin ligase and homologous recombination repair.* FEBS Lett, 2011. **585**(18): p. 2836-44.
24. Shanbhag, N.M., et al., *ATM-dependent chromatin changes silence transcription in cis to DNA double-strand breaks.* Cell, 2010. **141**(6): p. 970-81.
25. Ginjala, V., et al., *BMI1 is recruited to DNA breaks and contributes to DNA damage-induced H2A ubiquitination and repair.* Mol Cell Biol, 2011. **31**(10): p. 1972-82.
26. Goodarzi, A.A., et al., *ATM signaling facilitates repair of DNA double-strand breaks associated with heterochromatin.* Mol Cell, 2008. **31**(2): p. 167-77.
27. Chiolo, I., et al., *Double-strand breaks in heterochromatin move outside of a dynamic HP1a domain to complete recombinational repair.* Cell, 2011. **144**(5): p. 732-44.
28. Echalier, G. and A. Ohanessian, *[Isolation, in tissue culture, of Drosophila melangaster cell lines].* C R Acad Sci Hebd Seances Acad Sci D, 1969. **268**(13): p. 1771-3.
29. Baldi, S. and P.B. Becker, *The variant histone H2A.V of Drosophila--three roles, two guises.* Chromosoma, 2013. **122**(4): p. 245-58.
30. Sadoni, N., et al., *Stable chromosomal units determine the spatial and temporal organization of DNA replication.* J Cell Sci, 2004. **117**(Pt 22): p. 5353-65.
31. Hiratani, I., et al., *Global reorganization of replication domains during embryonic stem cell differentiation.* PLoS Biol, 2008. **6**(10): p. e245.
32. Marechal, A. and L. Zou, *DNA damage sensing by the ATM and ATR kinases.* Cold Spring Harb Perspect Biol, 2013. **5**(9).
33. Gurley, L.R., et al., *Heterochromatin and histone phosphorylation.* Exp Cell Res, 1978. **111**(2): p. 373-83.

34. Jin, F., et al., *A high-resolution map of the three-dimensional chromatin interactome in human cells.* Nature, 2013. **503**(7475): p. 290-4.
35. Hsieh, T.H., et al., *Mapping Nucleosome Resolution Chromosome Folding in Yeast by Micro-C.* Cell, 2015. **162**(1): p. 108-19.
36. Mizuguchi, T., et al., *Cohesin-dependent globules and heterochromatin shape 3D genome architecture in S. pombe.* Nature, 2014.
37. Schoenfelder, S., et al., *Preferential associations between co-regulated genes reveal a transcriptional interactome in erythroid cells.* Nat Genet, 2010. **42**(1): p. 53-61.
38. Kagey, M.H., et al., *Mediator and cohesin connect gene expression and chromatin architecture.* Nature, 2010. **467**(7314): p. 430-5.
39. Li, H.B., et al., *Insulators target active genes to transcription factories and polycomb-repressed genes to polycomb bodies.* PLoS Genet, 2013. **9**(4): p. e1003436.
40. Zeman, M.K. and K.A. Cimprich, *Causes and consequences of replication stress.* Nat Cell Biol, 2014. **16**(1): p. 2-9.
41. Jiang, Y., et al., *Common fragile sites are characterized by histone hypoacetylation.* Hum Mol Genet, 2009. **18**(23): p. 4501-12.
42. Cole, H.A., B.H. Howard, and D.J. Clark, *Activation-induced disruption of nucleosome position clusters on the coding regions of Gcn4-dependent genes extends into neighbouring genes.* Nucleic Acids Res, 2011. **39**(22): p. 9521-35.
43. Fujita, N. and P.A. Wade, *Use of bifunctional cross-linking reagents in mapping genomic distribution of chromatin remodeling complexes.* Methods, 2004. **33**(1): p. 81-5.
44. Raab, J.R., et al., *Human tRNA genes function as chromatin insulators.* EMBO J, 2012. **31**(2): p. 330-50.
45. Savic, V., et al., *Chipping away at gamma-H2AX foci.* Cell Cycle, 2009. **8**(20): p. 3285-90.
46. Petermann, E., et al., *Hydroxyurea-stalled replication forks become progressively inactivated and require two different RAD51-mediated pathways for restart and repair.* Mol Cell. **37**(4): p. 492-502.
47. Fernandez-Capetillo, O., et al., *H2AX is required for chromatin remodeling and inactivation of sex chromosomes in male mouse meiosis.* Dev Cell, 2003. **4**(4): p. 497-508.
48. Tjong, H., et al., *Physical tethering and volume exclusion determine higher-order genome organization in budding yeast.* Genome Res, 2012. **22**(7): p. 1295-305.
49. Duina, A.A., M.E. Miller, and J.B. Keeney, *Budding yeast for budding geneticists: a primer on the Saccharomyces cerevisiae model system.* Genetics, 2014. **197**(1): p. 33-48.
50. Oakes, M., et al., *Mutational analysis of the structure and localization of the nucleolus in the yeast Saccharomyces cerevisiae.* J Cell Biol, 1998. **143**(1): p. 23-34.

51. Jin, Q.W., J. Fuchs, and J. Loidl, *Centromere clustering is a major determinant of yeast interphase nuclear organization.* J Cell Sci, 2000. **113 (Pt 11)**: p. 1903-12.
52. Duan, Z., et al., *A three-dimensional model of the yeast genome.* Nature, 2010. **465**(7296): p. 363-7.
53. Albert, B., et al., *Systematic characterization of the conformation and dynamics of budding yeast chromosome XII.* J Cell Biol, 2013. **202**(2): p. 201-10.
54. Wong, H., et al., *A predictive computational model of the dynamic 3D interphase yeast nucleus.* Curr Biol, 2012. **22**(20): p. 1881-90.
55. Ruben, G.J., et al., *Nucleoporin Mediated Nuclear Positioning and Silencing of HMR.* PLoS One, 2011. **6**(7): p. e21923.
56. Palladino, F., et al., *SIR3 and SIR4 proteins are required for the positioning and integrity of yeast telomeres.* Cell, 1993. **75**: p. 543-555.
57. Taddei, A., et al., *Separation of silencing from perinuclear anchoring functions in yeast Ku80, Sir4 and Esc1 proteins.* Embo J, 2004. **23**(6): p. 1301-12.
58. Taddei, A., et al., *Multiple pathways tether telomeres and silent chromatin at the nuclear periphery: functional implications for sir-mediated repression.* Novartis Found Symp, 2005. **264**: p. 140-56; discussion 156-65, 227-30.
59. Bystricky, K., et al., *Chromosome looping in yeast: telomere pairing and coordinated movement reflect anchoring efficiency and territorial organization.* J Cell Biol, 2005. **168**(3): p. 375-87.
60. Pillus, L. and J. Rine, *Epigenetic inheritance of transcriptional states in S. cerevisiae.* Cell, 1989. **59**(4): p. 637-47.
61. Meluh, P.B. and D. Koshland, *Budding yeast centromere composition and assembly as revealed by in vivo cross-linking.* Genes Dev, 1997. **11**(24): p. 3401-12.
62. Belagal, P., et al., *Decoding the principles underlying the frequency of association with nucleoli for RNA polymerase III-transcribed genes in budding yeast.* Mol Biol Cell, 2016. **27**(20): p. 3164-3177.
63. Dekker, J., et al., *Capturing chromosome conformation.* Science, 2002. **295**(5558): p. 1306-11.
64. Zhao, Z., et al., *Circular chromosome conformation capture (4C) uncovers extensive networks of epigenetically regulated intra- and interchromosomal interactions.* Nat Genet, 2006. **38**(11): p. 1341-7.
65. Rao, S.S., et al., *A 3D Map of the Human Genome at Kilobase Resolution Reveals Principles of Chromatin Looping.* Cell, 2014. **159**(7): p. 1665-80.
66. Mercy, G., et al., *3D organization of synthetic and scrambled chromosomes.* Science, 2017. **355**(6329).
67. Jin, Q., et al., *Yeast nuclei display prominent centromere clustering that is reduced in nondividing cells and in meiotic prophase.* J Cell Biol, 1998. **141**(1): p. 21-9.

68. Heidinger-Pauli, J.M., et al., *Systematic reduction of cohesin differentially affects chromosome segregation, condensation, and DNA repair.* Curr Biol, 2010. **20**(10): p. 957-63.
69. D'Ambrosio, C., et al., *Identification of cis-acting sites for condensin loading onto budding yeast chromosomes.* Genes Dev, 2008. **22**(16): p. 2215-27.
70. Ocampo-Hafalla, M.T. and F. Uhlmann, *Cohesin loading and sliding.* J Cell Sci, 2011. **124**(Pt 5): p. 685-91.
71. Ocampo-Hafalla, M., et al., *Evidence for cohesin sliding along budding yeast chromosomes.* Open Biol, 2016. **6**(6).
72. Lopez-Serra, L., et al., *The Scc2-Scc4 complex acts in sister chromatid cohesion and transcriptional regulation by maintaining nucleosome-free regions.* Nat Genet, 2014. **46**(10): p. 1147-51.
73. Glynn, E.F., et al., *Genome-wide mapping of the cohesin complex in the yeast Saccharomyces cerevisiae.* PLoS Biol, 2004. **2**(9): p. E259.
74. Tanaka, T., et al., *Identification of cohesin association sites at centromeres and along chromosome arms.* Cell, 1999. **98**(6): p. 847-58.
75. Tanaka, T., et al., *Cohesin ensures bipolar attachment of microtubules to sister centromeres and resists their precocious separation.* Nat Cell Biol, 2000. **2**(8): p. 492-9.
76. Dubey, R.N. and M.R. Gartenberg, *A tDNA establishes cohesion of a neighboring silent chromatin domain.* Genes Dev, 2007. **21**(17): p. 2150-60.
77. Bausch, C., et al., *Transcription alters chromosomal locations of cohesin in Saccharomyces cerevisiae.* Mol Cell Biol, 2007. **27**(24): p. 8522-32.
78. Snider, C.E., et al., *Dyskerin, tRNA genes, and condensin tether pericentric chromatin to the spindle axis in mitosis.* J Cell Biol, 2014. **207**(2): p. 189-99.
79. Chang, C.R., et al., *Targeting of cohesin by transcriptionally silent chromatin.* Genes Dev, 2005. **19**(24): p. 3031-42.
80. Hirano, T. and T.J. Mitchison, *A heterodimeric coiled-coil protein required for mitotic chromosome condensation in vitro.* Cell, 1994. **79**: p. 449-458.
81. Hirano, T., *Condensins: universal organizers of chromosomes with diverse functions.* Genes Dev, 2012. **26**(15): p. 1659-78.
82. Donze, D., et al., *The boundaries of the silenced HMR domain in Saccharomyces cerevisiae.* Genes Dev, 1999. **13**(6): p. 698-708.
83. Dhillon, N., et al., *DNA polymerase epsilon, acetylases and remodellers cooperate to form a specialized chromatin structure at a tRNA insulator.* Embo J, 2009. **28**(17): p. 2583-600.
84. Chen, M. and M.R. Gartenberg, *Coordination of tRNA transcription with export at nuclear pore complexes in budding yeast.* Genes Dev, 2014. **28**(9): p. 959-70.
85. Thompson, M., et al., *Nucleolar clustering of dispersed tRNA genes.* Science, 2003. **302**(5649): p. 1399-401.
86. Haeusler, R.A., et al., *Clustering of yeast tRNA genes is mediated by specific association of condensin with tRNA gene transcription complexes.* Genes Dev, 2008. **22**(16): p. 2204-14.

87. Taddei, A., H. Schober, and S.M. Gasser, *The budding yeast nucleus.* Cold Spring Harb Perspect Biol, 2010. **2**(8): p. a000612.
88. Zimmer, C. and E. Fabre, *Principles of chromosomal organization: lessons from yeast.* J Cell Biol, 2011. **192**(5): p. 723-33.
89. Palladino, F., et al., *The positioning of yeast telomeres depends on SIR3, SIR4, and the integrity of the nuclear membrane.* Cold Spring Harb Symp Quant Biol, 1993. **58**: p. 733-46.
90. Fabre, E. and M. Spichal, *Subnuclear Architecture of telomeres and subtelomeres in yeast*, in *SubTelomeres*, E.J. Louis and M.M. Becker, Editors. 2014, Springer. p. 13-37.
91. Andrulis, E.D., et al., *Esc1, a nuclear periphery protein required for Sir4-based plasmid anchoring and partitioning.* Mol Cell Biol, 2002. **22**(23): p. 8292-301.
92. Bupp, J.M., et al., *Telomere anchoring at the nuclear periphery requires the budding yeast Sad1-UNC-84 domain protein Mps3.* J Cell Biol, 2007. **179**(5): p. 845-54.
93. Mekhail, K., et al., *Role for perinuclear chromosome tethering in maintenance of genome stability.* Nature, 2008. **456**(7222): p. 667-70.
94. Klein, F., et al., *Localization of RAP1 and topoisomerase II in nuclei and meiotic chromosomes of yeast.* J Cell Biol, 1992. **117**(5): p. 935-48.
95. Taddei, A., et al., *Nuclear pore association confers optimal expression levels for an inducible yeast gene.* Nature, 2006. **441**(7094): p. 774-8.
96. Dieci, G., et al., *The expanding RNA polymerase III transcriptome.* Trends Genet, 2007.
97. Oki, M. and R.T. Kamakaka, *Barrier Function at HMR.* Mol Cell, 2005. **19**(5): p. 707-16.
98. Weiner, A., et al., *High-resolution nucleosome mapping reveals transcription-dependent promoter packaging.* Genome Res, 2010. **20**(1): p. 90-100.
99. Yuan, G.C., et al., *Genome-scale identification of nucleosome positions in S. cerevisiae.* Science, 2005. **309**(5734): p. 626-30.
100. Cole, H.A., B.H. Howard, and D.J. Clark, *Genome-wide mapping of nucleosomes in yeast using paired-end sequencing.* Methods Enzymol, 2012. **513**: p. 145-68.
101. Geiduschek, E.P. and G.A. Kassavetis, *The RNA polymerase III transcription apparatus.* J Mol Biol, 2001. **310**(1): p. 1-26.
102. Schramm, L. and N. Hernandez, *Recruitment of RNA polymerase III to its target promoters.* Genes Dev, 2002. **16**(20): p. 2593-620.
103. Ng, H.H., et al., *Genome-wide location and regulated recruitment of the RSC nucleosome-remodeling complex.* Genes Dev, 2002. **16**(7): p. 806-19.
104. Damelin, M., et al., *The genome-wide localization of Rsc9, a component of the RSC chromatin-remodeling complex, changes in response to stress.* Mol Cell, 2002. **9**(3): p. 563-73.
105. Frenkel, F.E., et al., *Evolution of tRNA-like sequences and genome variability.* Gene, 2004. **335**: p. 57-71.

106. Goodenbour, J.M. and T. Pan, *Diversity of tRNA genes in eukaryotes.* Nucleic Acids Res, 2006. **34**(21): p. 6137-46.
107. Withers, M., L. Wernisch, and M. dos Reis, *Archaeology and evolution of transfer RNA genes in the Escherichia coli genome.* Rna, 2006. **12**(6): p. 933-42.
108. Wang, J., V.V. Lunyak, and I.K. Jordan, *Genome-wide prediction and analysis of human chromatin boundary elements.* Nucleic Acids Res, 2012. **40**(2): p. 511-29.
109. Van Bortle, K. and V.G. Corces, *tDNA insulators and the emerging role of TFIIIC in genome organization.* Transcription, 2012. **3**(6): p. 277-84.
110. Kirkland, J.G., J.R. Raab, and R.T. Kamakaka, *TFIIIC bound DNA elements in nuclear organization and insulation.* Biochim Biophys Acta, 2013. **1829**(3-4): p. 418-24.
111. Biswas, M., et al., *Limiting the extent of the RDN1 heterochromatin domain by a silencing barrier and Sir2 protein levels in Saccharomyces cerevisiae.* Mol Cell Biol, 2009. **29**(10): p. 2889-98.
112. Korde, A., J.M. Rosselot, and D. Donze, *Intergenic Transcriptional Interference Is Blocked by RNA Polymerase III Transcription Factor TFIIIB in Saccharomyces cerevisiae.* Genetics, 2013. **196**(2): p. 427-38.
113. Simms, T.A., et al., *The Saccharomyces cerevisiae TRT2 tRNAThr gene upstream of STE6 is a barrier to repression in MATalpha cells and exerts a potential tRNA position effect in MATa cells.* Nucleic Acids Res, 2004. **32**(17): p. 5206-13.
114. Simms, T.A., et al., *TFIIIC binding sites function as both heterochromatin barriers and chromatin insulators in Saccharomyces cerevisiae.* Eukaryot Cell, 2008. **7**(12): p. 2078-86.
115. Van Bortle, K., et al., *Insulator function and topological domain border strength scale with architectural protein occupancy.* Genome Biol, 2014. **15**(6): p. R82.
116. Ebersole, T., et al., *tRNA genes protect a reporter gene from epigenetic silencing in mouse cells.* Cell Cycle, 2011. **10**(16): p. 2779-91.
117. Pombo, A., et al., *Regional specialization in human nuclei: visualization of discrete sites of transcription by RNA polymerase III.* Embo J, 1999. **18**(8): p. 2241-53.
118. Haeusler, R.A. and D.R. Engelke, *Spatial organization of transcription by RNA polymerase III.* Nucleic Acids Res, 2006. **34**(17): p. 4826-36.
119. Noma, K., et al., *A role for TFIIIC transcription factor complex in genome organization.* Cell, 2006. **125**(5): p. 859-72.
120. Iwasaki, O., et al., *Centromeric localization of dispersed Pol III genes in fission yeast.* Mol Biol Cell, 2010. **21**(2): p. 254-65.
121. Nemeth, A., et al., *Initial genomics of the human nucleolus.* PLoS Genet, 2010. **6**(3): p. e1000889.

122. Hou, C., et al., *Gene density, transcription, and insulators contribute to the partition of the Drosophila genome into physical domains.* Mol Cell, 2012. **48**(3): p. 471-84.
123. Kogut, I., et al., *The Scc2/Scc4 cohesin loader determines the distribution of cohesin on budding yeast chromosomes.* Genes Dev, 2009. **23**(19): p. 2345-57.
124. Huang, J. and B.C. Laurent, *A Role for the RSC chromatin remodeler in regulating cohesion of sister chromatid arms.* Cell Cycle, 2004. **3**(8): p. 973-5.
125. Ho, C.K. and J. Abelson, *Testing for intron function in the essential Saccharomyces cerevisiae tRNA(SerUCG) gene.* J Mol Biol, 1988. **202**(3): p. 667-72.
126. Dion, V., et al., *Increased mobility of double-strand breaks requires Mec1, Rad9 and the homologous recombination machinery.* Nat Cell Biol, 2012.
127. Mine-Hattab, J. and R. Rothstein, *Increased chromosome mobility facilitates homology search during recombination.* Nat Cell Biol, 2012.
128. Verdaasdonk, J.S., et al., *Centromere tethering confines chromosome domains.* Mol Cell, 2013. **52**(6): p. 819-31.
129. Hsieh, T.S., et al., *Micro-C XL: assaying chromosome conformation from the nucleosome to the entire genome.* Nat Methods, 2016. **13**(12): p. 1009-1011.
130. Guacci, V., E. Hogan, and D. Koshland, *Centromere position in budding yeast: evidence for anaphase A.* Mol Biol Cell, 1997. **8**(6): p. 957-72.
131. Miele, A., K. Bystricky, and J. Dekker, *Yeast silent mating type loci form heterochromatic clusters through silencer protein-dependent long-range interactions.* PLoS Genet, 2009. **5**(5): p. e1000478.
132. Donze, D. and R.T. Kamakaka, *RNA polymerase III and RNA polymerase II promoter complexes are heterochromatin barriers in Saccharomyces cerevisiae.* Embo J, 2001. **20**(3): p. 520-31.
133. Mano, Y., et al., *Single cell visualization of yeast gene expression shows correlation of epigenetic switching between multiple heterochromatic regions through multiple generations.* PLoS Biol, 2013. **11**(7): p. e1001601.
134. Valenzuela, L., S. Gangadharan, and R.T. Kamakaka, *Analyses of SUM1-1-mediated long-range repression.* Genetics, 2006. **172**(1): p. 99-112.
135. Valenzuela, L., et al., *Long-range communication between the silencers of HMR.* Mol Cell Biol, 2008. **28**(6): p. 1924-35.
136. Roberts, D.N., et al., *The RNA polymerase III transcriptome revealed by genome-wide localization and activity-occupancy relationships.* Proc Natl Acad Sci U S A, 2003. **100**(25): p. 14695-700.
137. Moqtaderi, Z. and K. Struhl, *Genome-wide occupancy profile of the RNA polymerase III machinery in Saccharomyces cerevisiae reveals loci with incomplete transcription complexes.* Mol Cell Biol, 2004. **24**(10): p. 4118-27.
138. Harismendy, O., et al., *Genome-wide location of yeast RNA polymerase III transcription machinery.* Embo J, 2003. **22**(18): p. 4738-47.

139. Fu, Y., et al., *The insulator binding protein CTCF positions 20 nucleosomes around its binding sites across the human genome.* PLoS Genet, 2008. **4**(7): p. e1000138.
140. Dion, M.F., et al., *Dynamics of replication-independent histone turnover in budding yeast.* Science, 2007. **315**(5817): p. 1405-8.
141. Nagarajavel, V., et al., *Global 'bootprinting' reveals the elastic architecture of the yeast TFIIIB-TFIIIC transcription complex in vivo.* Nucleic Acids Res, 2013. **41**(17): p. 8135-43.
142. Kornberg, R., *The location of nucleosomes in chromatin: specific or statistical.* Nature, 1981. **292**(5824): p. 579-80.
143. Baetz, K.K., et al., *The ctf13-30/CTF13 genomic haploinsufficiency modifier screen identifies the yeast chromatin remodeling complex RSC, which is required for the establishment of sister chromatid cohesion.* Mol Cell Biol, 2004. **24**(3): p. 1232-44.
144. Blat, Y. and N. Kleckner, *Cohesins bind to preferential sites along yeast chromosome III, with differential regulation along arms versus the centric region.* Cell, 1999. **98**(2): p. 249-59.
145. Laloraya, S., V. Guacci, and D. Koshland, *Chromosomal addresses of the cohesin component Mcd1p.* J Cell Biol, 2000. **151**(5): p. 1047-56.
146. Lindroos, H.B., et al., *Chromosomal association of the Smc5/6 complex reveals that it functions in differently regulated pathways.* Mol Cell, 2006. **22**(6): p. 755-67.
147. Klein, F., et al., *A central role for cohesins in sister chromatid cohesion, formation of axial elements, and recombination during yeast meiosis.* Cell, 1999. **98**(1): p. 91-103.
148. Kitada, T., et al., *gammaH2A is a component of yeast heterochromatin required for telomere elongation.* Cell Cycle, 2011. **10**(2): p. 293-300.
149. Raab, J.R. and R.T. Kamakaka, *Insulators and promoters: closer than we think.* Nat Rev Genet, 2010. **11**(6): p. 439-46.
150. Gehlen, L.R., et al., *Chromosome positioning and the clustering of functionally related loci in yeast is driven by chromosomal interactions.* Nucleus, 2012. **3**(4): p. 370-83.
151. Dujon, B., *The yeast genome project: what did we learn?* Trends in Genet., 1996. **12**(7): p. 263-270.
152. Sharp, P.M. and A.T. Lloyd, *Regional base composition variation along yeast chromosome III: evolution of chromosome primary structure.* Nucleic Acids Res, 1993. **21**(2): p. 179-83.
153. Dekker, J., *GC- and AT-rich chromatin domains differ in conformation and histone modification status and are differentially modulated by Rpd3p.* Genome Biol, 2007. **8**(6): p. R116.
154. Blat, Y., et al., *Physical and functional interactions among basic chromosome organizational features govern early steps of meiotic chiasma formation.* Cell, 2002. **111**(6): p. 791-802.

155. Baudat, F. and A. Nicolas, *Clustering of meiotic double-strand breaks on yeast chromosome III.* Proc Natl Acad Sci U S A, 1997. **94**(10): p. 5213-8.
156. Gerton, J.L., et al., *Global mapping of meiotic recombination hotspots and coldspots in the yeast Saccharomyces cerevisiae.* Proc Natl Acad Sci U S A, 2000. **97**(21): p. 11383-90.
157. Casolari, J.M., et al., *Genome-wide localization of the nuclear transport machinery couples transcriptional status and nuclear organization.* Cell, 2004. **117**(4): p. 427-39.
158. Bystricky, K., et al., *Long-range compaction and flexibility of interphase chromatin in budding yeast analyzed by high-resolution imaging techniques.* Proc Natl Acad Sci U S A, 2004. **101**(47): p. 16495-500.
159. Gartenberg, M.R., et al., *Sir-mediated repression can occur independently of chromosomal and subnuclear contexts.* Cell, 2004. **119**(7): p. 955-67.
160. Taddei, A. and S.M. Gasser, *Multiple pathways for telomere tethering: functional implications of subnuclear position for heterochromatin formation.* Biochim Biophys Acta, 2004. **1677**(1-3): p. 120-8.
161. Schober, H., et al., *Yeast telomerase and the SUN domain protein Mps3 anchor telomeres and repress subtelomeric recombination.* Genes Dev, 2009. **23**(8): p. 928-38.
162. Therizols, P., et al., *Chromosome arm length and nuclear constraints determine the dynamic relationship of yeast subtelomeres.* Proc Natl Acad Sci U S A, 2010. **107**(5): p. 2025-30.
163. Gartenberg, M.R. and J.S. Smith, *The Nuts and Bolts of Transcriptionally Silent Chromatin in Saccharomyces cerevisiae.* Genetics, 2016. **203**(4): p. 1563-99.
164. Dodson, A.E. and J. Rine, *Heritable capture of heterochromatin dynamics in Saccharomyces cerevisiae.* Elife, 2015. **4**: p. e05007.
165. Mahoney, D.J., et al., *Mutations in the HML E silencer of Saccharomyces cerevisiae yield metastable inheritance of transcriptional repression.* Genes and Dev., 1991. **5**: p. 605-615.
166. Sussel, L., D. Vannier, and D. Shore, *Epigenetic switching of transcriptional states: cis- and trans-acting factors affecting establishment of silencing at the HMR locus in Saccharomyces cerevisiae.* Mol Cell Biol, 1993. **13**(7): p. 3919-28.
167. Xu, E.Y., K.A. Zawadzki, and J.R. Broach, *Single-cell observations reveal intermediate transcriptional silencing states.* Mol Cell, 2006. **23**(2): p. 219-29.
168. Holmes, S.C. and J.R. Broach, *Silencers are required for inheritance of the repressed state in yeast.* Genes and Dev., 1996. **10**: p. 1021-1032.
169. Cheng, T.H. and M.R. Gartenberg, *Yeast heterochromatin is a dynamic structure that requires silencers continuously.* Genes Dev, 2000. **14**(4): p. 452-63.
170. Fourel, G., E. Lebrun, and E. Gilson, *Protosilencers as building blocks for heterochromatin.* Bioessays, 2002. **24**(9): p. 828-35.

171. Lebrun, E., et al., *Protosilencers in Saccharomyces cerevisiae subtelomeric regions.* Genetics, 2001. **158**(1): p. 167-76.
172. Gasser, S.M., et al., *The function of telomere clustering in yeast: the circe effect.* Cold Spring Harb Symp Quant Biol, 2004. **69**: p. 327-37.
173. Wang, Y., M. Vujcic, and D. Kowalski, *DNA replication forks pause at silent origins near the HML locus in budding yeast.* Mol Cell Biol, 2001. **21**(15): p. 4938-48.
174. Lemoine, F.J., et al., *Chromosomal translocations in yeast induced by low levels of DNA polymerase a model for chromosome fragile sites.* Cell, 2005. **120**(5): p. 587-98.
175. Ivessa, A.S., et al., *The Saccharomyces cerevisiae helicase Rrm3p facilitates replication past nonhistone protein-DNA complexes.* Mol Cell, 2003. **12**(6): p. 1525-36.
176. Admire, A., et al., *Cycles of chromosome instability are associated with a fragile site and are increased by defects in DNA replication and checkpoint controls in yeast.* Genes Dev, 2006. **20**(2): p. 159-73.
177. Deshpande, A.M. and C.S. Newlon, *DNA replication fork pause sites dependent on transcription.* Science, 1996. **272**(5264): p. 1030-3.
178. Azvolinsky, A., et al., *Highly transcribed RNA polymerase II genes are impediments to replication fork progression in Saccharomyces cerevisiae.* Mol Cell, 2009. **34**(6): p. 722-34.
179. Keogh, M.C., et al., *A phosphatase complex that dephosphorylates gammaH2AX regulates DNA damage checkpoint recovery.* Nature, 2006. **439**(7075): p. 497-501.
180. Chen, L.L. and L. Yang, *ALUternative Regulation for Gene Expression.* Trends Cell Biol, 2017.
181. Lunyak, V.V., et al., *Developmentally regulated activation of a SINE B2 repeat as a domain boundary in organogenesis.* Science, 2007. **317**(5835): p. 248-51.
182. Casper, A.M., et al., *ATR regulates fragile site stability.* Cell, 2002. **111**(6): p. 779-89.
183. Glover, T.W., et al., *Mechanisms of common fragile site instability.* Hum Mol Genet, 2005. **14 Spec No. 2**: p. R197-205.
184. Miller, C.T., et al., *Genomic amplification of MET with boundaries within fragile site FRA7G and upregulation of MET pathways in esophageal adenocarcinoma.* Oncogene, 2006. **25**(3): p. 409-18.
185. Mirkin, E.V. and S.M. Mirkin, *Replication fork stalling at natural impediments.* Microbiol Mol Biol Rev, 2007. **71**(1): p. 13-35.
186. Voineagu, I., et al., *Replication stalling at unstable inverted repeats: interplay between DNA hairpins and fork stabilizing proteins.* Proc Natl Acad Sci U S A, 2008. **105**(29): p. 9936-41.
187. Boeke, J.D., et al., *GENOME ENGINEERING. The Genome Project-Write.* Science, 2016. **353**(6295): p. 126-7.

188. Cole, H.A., et al., *Heavy transcription of yeast genes correlates with differential loss of histone H2B relative to H4 and queued RNA polymerases.* Nucleic Acids Res, 2014. **42**(20): p. 12512-22.
189. Ocampo, J., et al., *The ISW1 and CHD1 ATP-dependent chromatin remodelers compete to set nucleosome spacing in vivo.* Nucleic Acids Res, 2016. **44**(10): p. 4625-35.
190. Langmead, B. and S.L. Salzberg, *Fast gapped-read alignment with Bowtie 2.* Nat Methods, 2012. **9**(4): p. 357-9.
191. Heun, P., et al., *Chromosome dynamics in the yeast interphase nucleus.* Science, 2001. **294**(5549): p. 2181-6.